

# We are IntechOpen, the world's leading publisher of Open Access books Built by scientists, for scientists

5,800

Open access books available

142,000

International authors and editors

180M

Downloads

Our authors are among the

154

Countries delivered to

TOP 1%

most cited scientists

12.2%

Contributors from top 500 universities



WEB OF SCIENCE™

Selection of our books indexed in the Book Citation Index  
in Web of Science™ Core Collection (BKCI)

Interested in publishing with us?  
Contact [book.department@intechopen.com](mailto:book.department@intechopen.com)

Numbers displayed above are based on latest data collected.  
For more information visit [www.intechopen.com](http://www.intechopen.com)



# Additive Manufactured Zirconia-Based Bio-Ceramics for Biomedical Applications

*Sakthiabirami Kumaresan, Soundharrajan Vaiyapuri, Jin-Ho Kang, Nileshkumar Dubey, Geetha Manivasagam, Kwi-Dug and Sang-Won Park*

## Abstract

Zirconia was established as one of the chief vital ceramic materials for its superior mechanical permanency and biocompatibility, which make it a popular material for dental and orthopedic applications. This has inspired biomedical engineers to exploit zirconia-based bioceramics for dental restorations and repair of load-bearing bone defects caused by cancer, arthritis, and trauma. Additive manufacturing (AM) is being promoted as a possible technique for mimicking the complex architecture of human tissues, and advancements reported in the recent past make it a suitable choice for clinical applications. AM is a bottom-up approach that can offer a high resolution to 3D printed zirconia-based bioceramics for implants, prostheses, and scaffold manufacturing. Substantial research has been initiated worldwide on a large scale for reformatting and optimizing zirconia bioceramics for biomedical applications to maximize the clinical potential of AM. This book chapter provides a comprehensive summary of zirconia-based bioceramics using AM techniques for biomedical applications and highlights the challenges related to AM of zirconia.

**Keywords:** additive manufacturing (AM), zirconia, dental restorations, scaffolds, implants, challenges

## 1. Introduction

The use of biomaterials in the reconstruction of injured body parts and skeletal healing is unavoidable. Diverse biomaterials including ceramics, metals, polymers, hydrogels, and composites are explored and have achieved clinical success as well [1–3]. For bone restoration applications ceramic biomaterials are well recognized by biomaterial engineers and medical experts due to their biocompatibility and osteoconductivity. Each bioceramic has its unique properties, and they can be divided into three categories based on the properties: [1] bioactive ceramics: capable of establishing chemical interaction with the cell surface, [2] bio-inert ceramics: fully unreactive to the living ecosystem, [3] resorbable bioceramics: undergoes in vivo deficiency for phagocytosis or dissolution of the biomaterials in human body fluids [4]. The standard bioactive ceramics used for bone-regeneration applications

are bio-glasses and calcium phosphate-based resources, such as beta-tricalcium phosphate, hydroxyapatite, and biphasic calcium phosphate (mixture of beta-tricalcium phosphate and hydroxyapatite). However, alumina and zirconia oxide are the well-established bio-inert ceramics used in classic bone-regeneration applications [5]. Each bioceramics are widely used in the various human parts restoration applications based on the needs and capabilities. Excellent mechanical stability and biocompatibility brand zirconia as a potential dental restoration and bone scaffold material for load-bearing applications [6]. Hence, rigorous efforts were concentrated on zirconia-based ceramics in recent times by medical and research experts for dental and biomedical applications.

### **1.1 Overview of zirconia**

Zirconia is a polycrystalline dioxide ceramic of the transition metal zirconium [3, 7]. It was originally documented in 1789 by Martin Heinrich Klaproth, a German chemist [8]. Zirconia exists in three distinct crystal structures depending on the pressure and temperature: monoclinic, tetragonal, and cubic structures [9]. The monoclinic crystal structure is more constant from room temperature to 1170°C, but it has inferior mechanical properties compared to the other two structures [10]. It is commonly accepted that the monoclinic structure will transform into a tetragonal structure during thermal treatment between 1170°C and 2370°C. This change in crystal structure is accompanied by measurable volume reductions (4–5%) during the cooling period [8]. If the temperature is increased further, the tetragonal structure shrinks to form a cubic structure (between 2370°C and 2680°C, the melting point). During cooling, a noticeable volume expansion of 3–4% was observed, which is attributable to the reversible transformation into the monoclinic crystal structure [9]. During phase transformation, internal stress is induced in the zirconia lattice, which results in crack propagation. To suppress the aforementioned behavior, several metallic oxides or dopants (stabilizing agents such as  $Y_2O_3$ ,  $MgO$ ,  $CaO$ , and  $CeO$ ) are added to stabilize the zirconia structure, and the resultant type of zirconia is known as partially stabilized zirconia (PSZ) [11].

The key features of PSZ are their ability to enhance the transformation toughening mechanism, which inhibits/shields the further propagation of cracks. Therefore, PSZ is considered suitable for biomedical applications in orthopedics and dentistry due to its unique toughening behavior. In the late 1970s, zirconia was widely used as an effective substitute material for metals and alumina in biomedical and dental applications. This was due to its long-lasting mechanical behaviors, such as good flexural strength and fracture resistance, admirable biocompatibility, chemical permanency, corrosion resistance, and esthetics [12, 13]. Nevertheless, the aging process of zirconia ceramic is stimulated by low-temperature degradation, which has unfavorable impacts on the mechanical strength of prostheses and subsequent growth of external flaws. The presence of microcracks may compromise the performance in the long term in biological fluids [14].

To date, zirconia-based materials have been used in numerous areas in the engineering (energy and aerospace), medicine (orthopedics), and dental (crowns and implants) fields [15]. Common categories of zirconia-based materials existing on the market for biomedical applications are yttrium tetragonal zirconia polycrystal (Y-TZP), glass-infiltrated zirconia-toughened alumina (ZTA), and magnesia partially stabilized zirconia (Mg-PSZ). The properties of these zirconia-based bioceramics are listed in **Table 1**.

In general, zirconia-based ceramics are manufactured using conventional fabrication techniques, such as injection molding [17], hot and cold isostatic pressing, and slip casting [18]. Digital techniques such as computer-aided design (CAD)

Properties	Y-TZP	ZTA	Mg-PSZ
Chemical constituents	Y <sub>2</sub> O <sub>3</sub> , ZrO <sub>2</sub>	Al <sub>2</sub> O <sub>3</sub> , ZrO <sub>2</sub>	MgO, ZrO <sub>2</sub>
Crystallinity	Monophasic	Biphasic	Biphasic
Density (g/cm <sup>3</sup> )	6.05	5	5
Flexural strength (MPa)	800–1300	750–850	700–800
Hardness (GPa)	10–12	12–15	5–6
Fracture toughness (MPa m <sup>1/2</sup> )	5–10	6–12	8–15

**Table 1.**  
 Properties of zirconia-based ceramics [16].

and computer-aided manufacturing (CAM) are extensively used to fabricate dental restorations [7, 19], as well as in subtractive manufacturing techniques, such as machining and milling. However, these techniques have limitations such as material wastage, difficulties in producing complex structures, being time consuming, and wearing of milling and cutting tools. Recently, additive manufacturing (AM) techniques have been increasingly used for the fabrication of high-potential complex ceramic parts with high precision and at reduced cost [20, 21]. Developments in AM technology for the fabrication of zirconia-based ceramic parts and their applications are discussed in the following section.

## 1.2 Additive manufacturing techniques

AM is one of the most widely used techniques in recent times, and it is capable of building three-dimensional (3D) complex geometric structures with high dimensional precision and within a short manufacturing time. 3D objects with high levels of complexity and structural architectures are fabricated by stacking up the materials layerwise using simulated design files [22, 23]. AM is also known as 3D printing, solid free-form fabrication, and rapid prototyping. The materials used for AM processes are in the form of powders, liquids, or solids. According to the ISO/ASTM 17296 standard, AM technology is mainly characterized into two types based on the degree of consolidation [24].

### 1.2.1 Single-step process or direct process

As the name suggests, the combined bulk product is manufactured with a basic/specified geometric shape in a single operation by melting and solidification or multi-pass welding (such as powder bed fusion, selective laser melting (SLM), or directed energy deposition), which is mostly used in metal AM.

### 1.2.2 Multistep or indirect process

It produces the products in multiple steps. First, the green body parts are constructed with the basic geometric shape by binding the powder particles with help of a polymer or binder. Subsequent steps include shape modification/densification, consolidation of the material, or modification of the material properties (such as binder jetting (BJ) and material extrusion). AM ceramics parts are typically formed using multistep progression [25].

For biomedical and dental applications, the 3D printing process principally comprises the following steps (precisely for clinical applications): 1. procurement of 3D models, 2. designing (CAD), 3. slicing, 4. 3D printing, and 5. postprocessing.

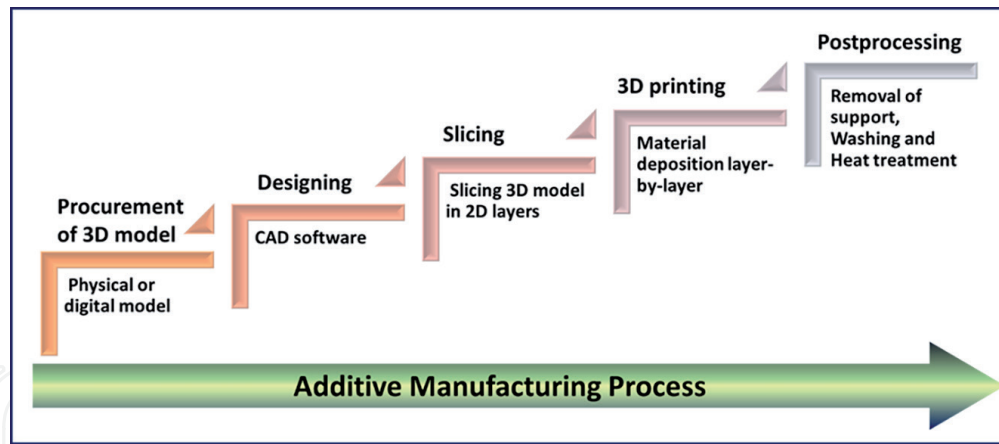


**Figure 1.**  
Illustration of additive manufacturing process.

Briefly, the AM process starts with the sorting of precise medical records (images) of the patients, which are obtained using computed tomography or magnetic resonance imaging. The procured data conforming to digital imaging and communications in medicine standards are transformed into digital models using materialise interactive medical image control system (MIMICS) or 3D DOCTOR software and formed into design files using 3D CAD software. The CAD file is converted to a standard tessellation language (.STL) file, and it is practically sliced to print patterns as per the specific needs of the implant. To acquire the desired print pattern of the products, numerous processing constraints such as printing speed, alignment, printing temperature, layer height, infill, laser condition, and environmental aspects are verified, based on experience or a literature review. The sliced file can be imported into the AM machine for printing/stacking the material in a layer, forming the 3D implant. Finally, the printed parts are exposed to washing, removal of sacrificial layer/support, and heat treatment [25, 26]. The detailed scheme of additive manufacturing process is displayed in **Figure 1**.

The most common AM technologies for the construction of high-strength ceramics are selective laser sintering/melting (SLS/SLM), stereolithography (SLA), digital light processing (DLP), binder jetting (BJ), fused deposition modeling (FDM), and direct ink writing (DIW) [27, 28]. Each AM technology has great commercial potential as well as limitations [29]. Likewise, additively manufactured

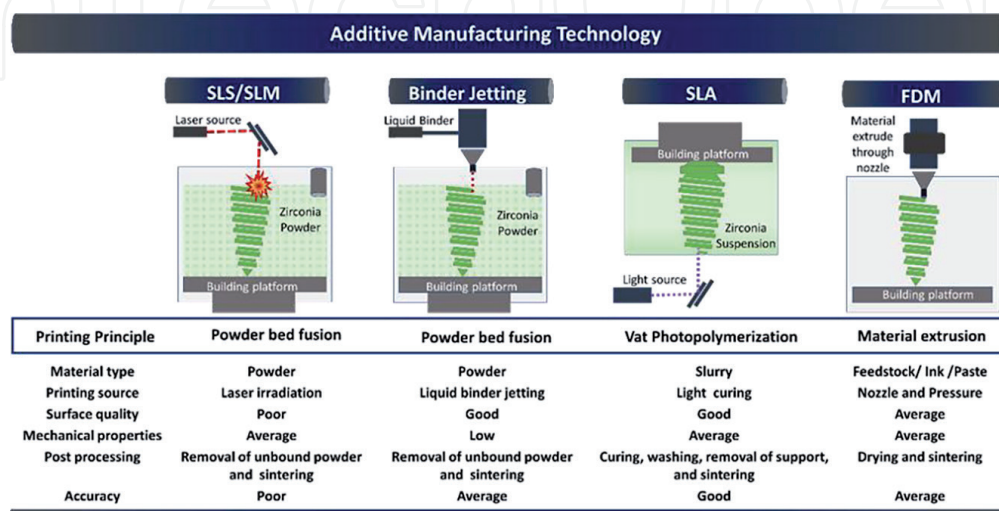


**Figure 2.**  
The schematic illustration of different types of AM technologies used for the fabrication of 3D zirconia-based ceramics.

zirconia-based ceramics have inferior mechanical properties due to the persistent porosity and flaw-sensitive properties of zirconia ceramics. Thus, acquiring mechanical properties equivalent to those of ceramics fabricated with more conventional approaches is a big challenge for ceramic AM [30]. However, the technology is still at an early stage, compared with conventional ceramic processing techniques [29]. It is widely recognized that ceramic materials possess a high melting point, high sinterability, and high vulnerability to thermal shock. Therefore, it is challenging to achieve fully consolidated parts, without shortcomings, using AM-based techniques that directly produce sintered objects [25]. To overcome these shortcomings, each AM technology adapts scientific strategies to construct zirconia-based ceramics with high accuracy and quality. In the following section, the formulation strategies of each AM technology are discussed. **Figure 2**, demonstrate the AM technologies used for the fabrication of zirconia parts.

## **2. Formulation and general properties of zirconia directed to biomedical applications**

### **2.1 Powder bed method**

#### *2.1.1 Selective laser sintering/melting (SLS/SLM)*

SLS technology uses a high-powered laser beam to sinter/fire the ceramics at an elevated temperature. The laser is aimed at specific areas of the aggregate powdered particles using the distribution to create solid objects [31–33]. The SLM is principally similar to SLS; however, SLM completely melts and fuses the powder particles using a high-powered laser beam to form a solid object [34, 35]. SLS/SLM is an AM technique that uses a laser and is based on the powder bed method that produces 3D solid structures either by sintering or melting the powder materials layerwise following an architecture based on CAD data. (Obtaining high-strength and high-density parts with a laser without debinding/sintering processes can facilitate effective and rapid fabrication, enabling the mass production of ceramic parts (direct AM process) [36, 37].

However, zirconia ceramic is difficult to handle with SLS/SLM, as it has a higher melting point than other bioceramics. In addition, reaching full densification and realizing crack-free final products made of ceramics-based materials using this process are still challenging. Therefore, several studies are investigating the effect of powder properties and processing parameters [21, 35, 38]. Researchers describe the effectiveness of pre-heating the powdered bed, which could improve the mechanical properties of the final ceramic object by reducing the thermal stress, which alleviates crack formation during printing [39, 40]. Most of the zirconia particles use 3–8 mol% yttria-stabilized zirconia (YSZ) to preserve the desired mechanical properties of a tetragonal phase at room temperature. Alternative approaches were also found to be effective in improving the mechanical properties of the zirconia. For example, composites comprising zirconia and alumina are also found to retain the tetragonal phase [40–42]. To improve the mechanical properties of the final zirconia part and prevent cracking, an indirect method in SLS/SLM has been developed and documented [42–44]. Specifically, ceramic powder particles are mixed/coated with a sacrificial polymer binder (which has a lower melting point than the ceramic) and the laser is targeted towards the powder, which melts and fuses the ceramic particles. The fused ceramic particles are then subjected to postprocessing (debinding and sintering) to attain the dense zirconia ceramic scaffolds [42]. The summary of zirconia-based ceramics printing configurations used in SLS/SLM methods is presented in **Table 2**.

Particle size ( $\mu\text{m}$ )	Powder composition	Laser & power	Post-processing	Ref.
1–4	Zircar ZYP-30 (10 wt%)	Phenix Systems PM100 (50 W) V = 1250–2000 mm/s	—	[35]
20–70	Alumina toughened zirconia (ATZ) (41.5, 80, 94) wt% ZrO <sub>2</sub> , (58.5, 20, 6) wt% Al <sub>2</sub> O <sub>3</sub>	Nd: YAG laser (150 W) for processing CO <sub>2</sub> laser (1000 W) for pre-heating	—	[45]
22.5–45	7Y-TZP (20–80 wt%)	MCP Realizer SLM 250, Germany	—	[40]
3–50	8Y-TZP + < 2 wt% graphite powder	Phenix ProX 200 Nd:YAG Laser power (W): 78–87	—	[46]
1–5	ATZ of Y-TZP (80 wt%)	CW 200 W Nd-YAG laser (redPOWER, SPI Lasers Ltd., UK) Laser power (W): 34	Post-thermal treatment at 1300°C for 2–10 h	[41]
—	ATZ of Y-TZP (80 wt%)	Realizer SLM 125 equipped with Nd:YAG laser Laser power (W): 90	—	[47]
—	3Y-TZP + 0.5 wt% MgO (magnesium oxide) powder +6.0 wt% epoxy resin	CO <sub>2</sub> laser ( $\lambda$ : 10.6 $\mu\text{m}$ ) with power of 100 W Laser power (W): 7	Cold isostatic pressing at 280 MPa	[44]
—	ZrO <sub>2</sub> + nylon 12	Energy density: 0.415 J/mm <sup>2</sup> Laser power: 6.6 W	Cold isostatic pressing at 200 MPa	[43]
—	3Y-TZP + isotactic polypropylene (PP)	CO <sub>2</sub> laser ( $\lambda$ : 10.6 $\mu\text{m}$ ) with power of 100 W	Warm isostatic pressing at 64 MPa Sintering in air at 1450°C for 2 h	[42]

**Table 2.** Summary of zirconia-based configurations used in SLS/SLM methods [34].

### 2.1.2 Binder jetting (BJ)

BJ is also based on the powder bed fusion technique, where a binder (binding agent) is selectively deposited to link powder materials. In this technique, a thin layer of ceramic material in powder form is evenly spread over the building platform with the help of a roller [48]. A binding ink is then sprayed onto the ceramic powder particles using the jetting head. The result is the ceramic powders and binders adhering together to form a solid structure. This is repeated multiple times and the layers are printed on top of each other to form the preferred 3D scaffolds. During printing, green ceramic parts are reinforced by boundless powder particles [24]. The BJ process can eliminate the internal residual stresses that evolve during building [1]. Moreover, the postprocessing steps such as the removal of unbound powders and sintering are conducted to consolidate the dense ceramic parts. The effective production of numerous ceramics such as hydroxyapatite, tricalcium phosphate, ZTA, and Al<sub>2</sub>O<sub>3</sub> structures with the required porosity using the BJ process have been reported in the literature for biomedical applications [49, 50]. However, obtaining the necessary shrinkage and density in the final product after sintering is still critical. Therefore, many researchers sought to address these issues

by integrating nanoparticles into the liquid binder. Recently Huang et al. [32] studied the use of an inorganic colloidal binder (decomposable binder) as a binding agent for the construction of 3Y-ZrO<sub>2</sub> ceramic structures using BJ technology. They selected zirconium basic carbonate as a precursor, and it was dispersed in the colloidal solvent to produce decomposable inorganic colloidal binder because it can be easily decomposed upon sintering and can form zirconia 3D parts with no residue [48]. It was established that the inorganic colloidal binder-based zirconia scaffolds exhibited superior surface quality and density compared to the conventional polymer binder. Conversely, Zhao et al. [32] \*\*\*attempted to print zirconia samples using a liquid binder containing zirconia nanoparticles (10 wt%). The density was increased by approximately 86.8%, whereas shrinkage was reduced by approximately 10.6% after sintering the printed parts [51].

## 2.2 Stereolithography

Among the AM technologies using zirconia, SLA technology is the most well-known and popular method. A photocurable resin comprising photopolymerizable monomers, a photoinitiator, and ceramic particles is molded into a slurry and selectively cured by ultraviolet (UV) radiation in sequential layers to build the 3D object with the desired shape [52]. The geometrical accuracy of the manufactured parts produced using SLA technology is dependent on the laser power, layer thickness, cure depth, and energy dose. The key steps in fabricating ceramic parts with complex geometries and high resolution using SLA are preparing a suitable photocurable ceramic suspension, building the ceramic part, and debinding and sintering [53]. One of the most important factors in this process is the properties of the ceramic suspension. Homogeneous dispersion of zirconia ceramic materials with raw resin is essential for establishing photocurable ceramic resins. The introduction of ceramic materials negatively impacts the properties of raw resin by increasing the viscosity and immobilizing the ceramic/resin suspension. To initiate a matrix around the ceramic materials during photopolymerization, a combination of monomers and oligomers is blended with the ceramic suspension as a binder [54]. It is essential to include a dispersant to prevent agglomerations and retain the resin stability. The dense ceramic parts fabrication is primarily dictated by the volume fraction of the ceramics. Increases in volume fraction improve the final properties of the product (porosity reduction, shrinkage reduction, strength improvement, crack/deformation suppression) [28]. Due to this unique characteristic, SLA-based printers are commercially available in different forms. Hence, design and materials engineers recommend altering the design and printing parameters to the finest quality using state-of-the-art techniques and materials. Many studies have been focused on advancing a suitable photocurable ceramic suspension for the fabrication of zirconia-based ceramic parts (**Table 3**).

### 2.2.1 Oligomers and monomers

The oligomer (prepolymer) applied to the zirconia in AM methods has a chain structure comprising a medium molecular weight monomer. The oligomer regulates the physical properties of the resin. The reactivity between the monomer and the polymer with a low molecular weight number influences the properties of the cured film through molecular bonding triggered by polymerization. The classification is based on the molecular structure and includes polyester, epoxy, urethane, polyether, and polyacrylic. In general, it is difficult to use the oligomers directly for AM due to their high viscosity [60, 61].



Particle size ( $\mu\text{m}$ )	Resin configuration	Solid loading (vol%)	Viscosity (Pa s)	Laser wavelength (nm)	Ref.
0.2	HDDA <sup>a</sup> + TMPTA <sup>a</sup>	55	1.65 at 200 s <sup>-1</sup>	—	[55]
—	HDDA + IBA <sup>a</sup> + PNPBDA <sup>a</sup>	58	9.02 at 5 s <sup>-1</sup>	375–425	[56]
0.2	AM <sup>b</sup> + MBAM <sup>b</sup> + Glycerol + Water	40	0.127	—	[57]
0.2	HDDA + PPTTA <sup>a</sup> + PEG <sup>c</sup> + U600 <sup>a</sup>	60 (wt%)	—	—	[58]
0.2	HDDA + PEGDA	83 (wt%)	1.23 at 100 s <sup>-1</sup>	405	[59]

<sup>a</sup>Acrylate-based monomer.  
<sup>b</sup>Acrylamide-based monomer.  
<sup>c</sup>Polyethylene glycol.

**Table 3.** Different formulations and viscosity characteristics for preparation of zirconia suspensions [53].

A monomer is a reactive diluent added to reduce the viscosity of an oligomer. The polymerization can be categorized into two types, namely, a free radical reaction or a cationic reaction [60, 62]. Acrylates and methacrylate are the most used monomers from free radical reactions [62]. Photopolymerization can be stimulated through a free radical initiator, and when the monomer receives a free radical from the initiator, it transfers the free radical to another monomer to form a polymer. The cationic reactive monomers can induce photopolymerization via cationic initiators. Monomers, such as epoxides, vinyl ethers, propenyl ethers, siloxanes, cyclic acetals, and furfurals, are capable of polymerization under a cationic mechanism. Epoxide is the preferred monomer from the cationic reaction groups [63].

### 2.2.2 Photoinitiator

Monomers and oligomers cannot independently initiate photopolymerization. Therefore, photoinitiators are added to generate reactive species that can trigger the monomers and oligomers. When polymerization is initiated, the reaction proceeds through a chain reaction of double bonds and forms a three-dimensional cross-linked bond together with reactive monomers and oligomers [64, 65]. Free radical photoinitiators added to certain monomers, such as acrylates and methacrylates, absorb UV light to generate free radicals and incite a double bond reaction of the monomers [66]. Cationic initiators can readily react with the binding of certain monomers, such as vinyl ethers and epoxides, because the absorbed UV light produces acids to induce polymerization of the monomers [63].

### 2.2.3 Dispersant

Dispersants are copolymers with soluble polymer chains and “fixing groups” that impart affinity to the surface of inorganic pigments such as zirconia [53]. The main mechanism in nonaqueous systems with low polarity is steric stabilization. Polymer chains are attached to the pigment surface by adsorption and form a brush-like layer that prevents re-agglomeration due to osmotic and entropy effects. The polymer chains of the dispersant are adsorbed onto the pigment surface to form a layer that prevents re-agglomeration. An effective layer typically ranges from 5 nm to 20 nm, with a particle diameter in the range of 0.05–1  $\mu\text{m}$ . Because the dispersant effects vary with the monomer and oligomer composition, as well as the properties

of the ceramic powder, care must be taken regarding the type and content of the dispersant.

### 2.3 Material extrusion

The compact ceramic raw material supplied to the extruder is difficult to use as an AM material because it has a high tendency of particle aggregation and, thus, increased resistance to flow [67]. Compatible ceramic powder and additives can guarantee permanency for storage and molding through homogeneous particle dispersion after mixing and, thus, facilitate the minimum pressure and viscosity for flow through the printing nozzle [68, 69].

Additionally, there is a need for good bonding and inhibition of separation between the deposited layers during printing [70, 71]. In addition, the included additives must be removed without defects during the post-treatment process [72, 73].

#### 2.3.1 Wax/thermoplastic base

A study on the composition of multicomponent additives for a wax/thermoplastic base is suggested in **Table 4**. In addition to the main additives (such as polyethylene), other components such as wax dispersants and plasticizers are also included to provide strength, elasticity, flexibility, plasticity, and lower viscosity [20].

#### 2.3.2 Water base

In the case of a feedstock in which a large amount of polymer is used as a dispersion medium, defects may occur during debinding after manufacturing. To solve this problem, an aqueous ceramic raw material is used. This water-based ceramic raw material enables the accumulation of zirconia powder with high content and decreases defects during degreasing due to the low content of organic matter.

Processes	Powder	State	Additive materials	Ref.
Wax & thermoplastic base	3 mol% YSZ 300 nm (40 vol%)	Feedstock	Low-density polyethene, paraffin wax, stearic acid	[74]
	3 mol% YSZ 90 nm (47 vol%)	Feedstock	High-density polyethylene, stearic acid, amorphous polyolefin, styrene-ethylene-butylene-styrene copolymer, paraffin wax, extender oil	[75]
	3 mol% YSZ 500 nm (85 wt%)	Feedstock	Ethylene-vinyl acetate copolymer, polyethylene, paraffin wax and stearic acid	[20]
Water base	3 mol% YSZ (45–50 vol%)	Paste	Anionic polyelectrolyte dispersant, hydroxypropyl methylcellulose, polyethyleneimine	[76]
	3 mol% YSZ 500 nm (50 vol%)	Paste	Water, acrylamide, N,N'-methylenebisacrylamide, ammonium citrate	[77]
	3 mol% YSZ 40 nm (60 vol%)	Paste	Ammonium polymethacrylate, methylcellulose, deionized water	[78]

**Table 4.**  
 Overview of extrusion processes for zirconia ceramics.

### **3. Biomedical application of AM zirconia**

#### **3.1 Dental applications**

The use of zirconia ceramic as a restorative material in the form of dental prostheses started in the early 1980s and gained considerable attention in the dental community, thereafter due to its unique properties (such as excellent esthetics including tooth-like color, high fracture toughness, flexural strength, corrosion resistance, and biocompatibility) [8]. Hence, it has become the best alternative for metal-based dental restorations. Zirconia ceramics have been used in dental applications in the form of dental crowns, dental implants, and fixed partial dentures since 1998 [19]. In general, zirconia restorations are fabricated using digital techniques, including subtractive manufacturing techniques such as CAD/CAM, which is the established method for producing fixed prosthetic restorations [79], where the milling machine is controlled by a computer numeric controlled system. The power-driven milling tools were used to mill/remove the material from a block (presintered or fully sintered ceramic block) to achieve the desired prosthesis background [80]. However, it has certain disadvantages during manufacturing, such as material wastage and wear of milling tools. In addition, its precision is limited, limiting object complexity, tooling equipment dimensions, material properties, among other problems [81]. AM incorporates recent advanced and evolving techniques in digital dentistry, which construct the three-dimensional component by layering the material. It is capable of making cost-effective customized dental prostheses with minimal material consumption and high precision [82]. However, research studies on the 3D printing of zirconia crowns and bridges for dental applications are limited. In addition, various issues such as poor geometrical accuracy, high porosity, and poor margins are unresolved. Recently, several research studies on 3D printing of zirconia ceramics using photopolymerization-based printing (SLA-based technologies) improved the effectiveness and accuracy, making the technique favorable.

##### *3.1.1 Restorative applications*

The goal of the dentist is to restore the lost tooth as naturally as possible. The most common material types used in the restorative field are metals and ceramics. However, ceramics possess significant advantages over metal/metal ceramics due to their natural appearance (tooth-like color), which satisfies the esthetic demands, making ceramics the material of choice [83, 84].

YSZ is the most widely used all-ceramic material in dental restorations due to its outstanding material properties [85]. It is used for load-bearing applications, such as dental crowns, bridges, veneers, and implant abutments. YSZ restorations have been used in clinical practice over the past two decades. It is used primarily as a core material for the fabrication of dental prosthesis frameworks. The chipping of ceramic veneers and fracture of the framework, when exposed to continuous masticatory load is often reported [86, 87]. For example, the thermal coefficients of the core material and outer veneer cap (porcelain/lithium disilicate) are different and subjected to different heat treatment temperatures that lead to catastrophic failure. Further, several other factors including surface treatment (airborne-particle abrasion/etching) of the framework and bond strength between the ceramics veneer and zirconia frameworks are consequential [9, 88].

The advancement in zirconia with full-contour monolithic zirconia restorations gained attention to address the aforementioned problems. The fabrication of crowns and bridges using monolithic zirconia is faster and cheaper compared to a manually constructed veneered prosthesis. In recent years, CAD/CAM technology

(subtractive) has been used for the fabrication of all-ceramic prostheses and abutments. The very attractive flexural strength and toughness of 3 mol% YSZ make it a classic and suitable material for dental use. Despite the promising properties of zirconia, the optical properties (translucency) are poor, i.e., it is opaque. Therefore, the larger esthetic-related issues initiated the demands for monolithic restorations. Dental material researchers and manufacturers have found several ways to increase translucency characteristics. The light transmission can be improved by either reducing the concentration of aluminum oxide or increasing the concentration of yttrium oxide [15]. For instance, the molar concentration of the yttria is varied (3–5%) to improve the translucency of zirconia with optimal mechanical properties. However, when the concentration of yttria is increased, the material exhibits higher translucency (more esthetics) but also exhibits a reduction in mechanical properties because the structural change into cubic phase becomes dominant. Evidently, the cubic phase does not allow transformation in crystal structure and this leads to a reduction in crack resistance. The “gradient technology” has become the modern advancement in the area of translucent zirconium oxide. A material-specific gradient is introduced into the milling block along with the color gradient (highly chromatic at the cervical region and less chromatic at the incisal region). In particular, the high-strength raw material 3Y-TZP is combined with the highly translucent raw material 5Y-TZP to create a continuous, layer-free color and translucent gradient [89]. The development of AM technology has attracted much attention to the fabrication of zirconia-based restoration with a high potential of making customized dental prosthesis with minimal waste (**Figure 3**).

In 2009, Ebert et al. [90] built a zirconia dental crown using the direct inkjet printing method. The printing ceramic suspension was loaded with 27 vol% of zirconia ceramics, with a relative density of 96.9%, flexural strength of 763 MPa, and a fracture toughness of 6.7 MPa m<sup>1/2</sup>. The printed and fired samples showed process-related defects, which were attributed to the clogging of the nozzles during printing that directly affected the mechanical properties. However, the authors demonstrated the potential to print 3D crowns using this technology. Likewise, Özkol et al. [91]

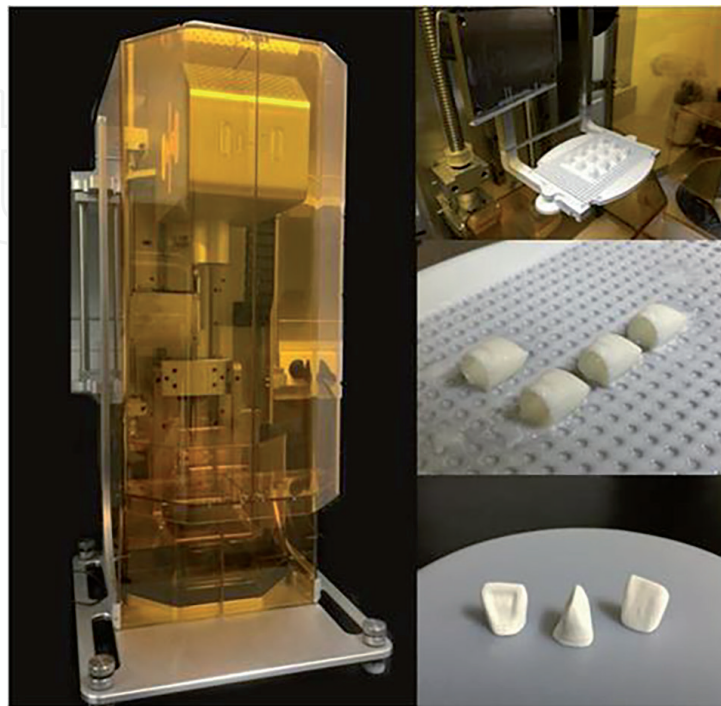


**Figure 3.**  
*AM zirconia crowns via DLP technology [56].*

Applications	Materials and ceramic content	Fabrication techniques	Density (%) and shrinkage (vol %)	Mechanical properties	Others	Ref.
Dental crown (2009)	YSZ 27 vol%	DIP (from Hewlett Packard)	Density 96.9% and Shrinkage 20%	Flexural strength 763 MPa; Weibull modulus 3.5; Fracture toughness 6.7 MPa m <sup>1/2</sup>	—	[90]
Dental crown (2011)	YSZ 47 vol%	Robo-casting	Shrinkage 30%	—	—	[92]
Dental bridge framework (2012)	YSZ (3Y-TZP) 40 vol%	DIP (from HP deskjet)	Density > 96%	Flexural strength-843 MPa; Weibull modulus 3.6; tensile strength-340 MPa	—	[91]
Dental bridges framework (2013)	ZTA (ZrO <sub>2</sub> -80% and Al <sub>2</sub> O <sub>3</sub> -20%)	SLM	Density-100%	Flexural strength 538 MPa	—	[45]
Dental bridges (2018)	YSZ 40 vol%	SLA (from Shaanxi Hengtong Intelligent Machine Co., Ltd.)	Density 98.58% and shrinkage 20–30%	Flexural strength 200.14 MPa; Vickers hardness 1398 HV	—	[57]
Dental crown (2018)	YSZ 37 vol%	SLA (polymer mold) and gel casting	Density 98.6% and Shrinkage 20.1%	Flexural strength 1170 MPa; Vickers hardness 1383 HV	—	[93]
Dental crown (2019)	YSZ	SLA (from 3DCeram)	—	—	Surface trueness of the 3D printed crown meets the requirement	[94]
Dental crown (2019)	YSZ 45 vol%	SLA (from Porimy 3D Printing Technology Co., Ltd.)	Density-5.83 g/cm <sup>3</sup> and Shrinkage 18.1% in length, 20% in width, and 24.3% in height.	Flexural strength 812 MPa; Weibull strength 866.7 MPa; Weibull modulus 7.44	Cement space 63.40 μm (occlusal area); 135.08 μm (axial area) and 169 μm (marginal area)	[95]
Implant-supported AM crown (2019)	Commercial slurry (3DMixZrO <sub>2</sub> )	SLA (from 3DCeram)	—	Fracture resistance 1243 N	—	[96]
Dental crown (2019)	YSZ (3Y-TZP) 48–58 vol%	DLP (from Octave Light R1)	Density 92.79% and Shrinkage—23.81%	Flexural strength 674.74 MPa	Geometrical overgrowth 36.94%	[56]

Applications	Materials and ceramic content	Fabrication techniques	Density (%) and shrinkage (vol %)	Mechanical properties	Others	Ref.
Dental crown (2020)	Commercial slurry (3DMixZrO <sub>2</sub> )	SLA (from 3DCeram)	—	—	Marginal and internal discrepancies	[97]
Occlusal veneers (2020)	YSZ 40–60 vol%	Litho-graphy-based ceramics manufacturing process (like DLP) (From Lithoz GmbH)	—	—	Load bearing capacity- Median Fmax values 2026 N	[98]
Dental crown (2020)	YSZ 50–55 vol%	Inkjet	Density 98.5%	Hardness 14.4 GPa; transverse rupture strength 520 MPa	—	[99]
Dental crown (2021)	Commercial slurry SL150	SLA (from Porimy 3D Printing Technology Co., Ltd.)	—	—	Dimensional accuracy 65 μm and marginal adaptation	[100]
Dental crown (2021)	Commercial slurry CSL150 (YSZ) 47 vol%	SLA (from Porimy 3D Printing Technology Co., Ltd.)	—	—	—	[101]
Dental prosthesis (bar shaped) (2021)	Commercial slurry (3DMixZrO <sub>2</sub> )	SLA (from 3DCeram)	—	Flexural strength 320.32 MPa and 281.12 MPa after aging; fracture resistance 640.64 N and 562.25 after aging	—	[102]
Dental prosthesis (bar shaped) (2021)	Commercial slurry (3DMixZrO <sub>2</sub> )	SLA (from 3DCeram)	Shrinkage—16.32% in length, 14.25% in width, and 20.33% in height.	—	—	[103]

**Table 5.**  
*AM zirconia for dental applications.*

attempted to print the zirconia bridge framework using a direct ink printing (DIP) method. The ceramic aqueous ink was prepared with 40 vol% solid content of 3Y-TZP. The printed components were dried and sintered at 1450°C. The relative density of the final product was >96%. Furthermore, finite element analysis was used to determine the stress distribution and the maximum tensile stress of the framework structure. The results of all different loading cases show hot spots on the bottom marginal area of the interdental connectors. The estimated maximum tensile stress values ranged between 250 and 350 MPa. The flexural strength was approximately 843 MPa (**Table 5**).

Lian et al. [57] reported that complex zirconia bridges were produced using the SLA technique with a high shape precision. They prepared a 40 vol% zirconia suspension and the laser scanning speed of 1200 mm/s was optimized for printing. The density and Vickers hardness of the sintered bridges was 98.58% and 1398 HV, respectively. Nevertheless, the flexural strength (200.14) was very low, and it was not good enough for actual dental applications, because of the internal defects formed during the printing process. The authors, therefore, suggested a study of the further optimization of the parameters of the SLA and sintering process. Additionally, in 2019 Wang et al. [94] conducted an in vitro experiment to investigate the surface trueness at different locations (external, intaglio, marginal, and occlusal) of 3D printed zirconia crowns constructed using SLA 3D printing technology.

The point-to-point difference between the scan data (3D printing) and corresponding CAD model data determines the trueness of the fabricated crown. The comparative color maps could demonstrate the accuracy and inaccuracy between the 3D printing and milling techniques. Meanwhile, Li et al. [95] examined the internal and marginal adaptation of 3D printed zirconia crowns and studied the physical and mechanical properties. The authors achieved a consistent flexural strength of 812 MPa and Weibull modulus of 7.44 by using 45 vol% zirconia suspensions. The mechanical strength is sufficient for dental crowns fabrication. While the cement spaces in occlusal (63.4), axial (134.08), and marginal (169.65) areas were not ideal for clinical applications, this can be attributed to light scattering and anisotropic sintering shrinkage.

However, in 2019 Jang et al. [56] investigated the microstructure and physical properties of zirconia products fabricated via DLP technology. The zirconia suspension was prepared using different volume fractions of the ceramic content from 48 vol% to 58 vol%. Cracks were observed on the zirconia specimens, and these cracks increased in number as the zirconia volume fraction decreased. The 3-point bending strength, relative density, and shrinkage of the printed samples were 674.74 MPa, 83.02%, and 23.81%, respectively. The maximum volume fraction possible for 3D printing was 58 vol%.

More recently in 2021, Zandinejad et al. [96] investigated the fracture resistance of AM zirconia crowns cemented to an implant-supported zirconia abutment. They also compared the AM zirconia crowns with milled zirconia, as well as lithium disilicate crowns. A universal testing machine at a crosshead speed of 2 mm/min was used to determine the fracture resistance, and it was verified that the fracture resistance of AM zirconia is equivalent to milled crowns. Nevertheless, intra-oral simulation research on the AM ceramic crowns should be conducted to authorize AM as a real-world technology for the construction of ceramic restorations in clinical dentistry.

### *3.1.2 Implant application*

The popularity of zirconia-based implants is growing enormously as an alternative to alumina and metal-based endosseous implants [104]. Since the late 1980s, zirconia has been used to build surgical implants for the replacement of total hip prostheses in orthopedic surgery [105]. Zirconia-based ceramics have superior mechanical properties and corrosion resistance [106]. Besides, in vitro and in vivo,

clinical studies of zirconia implants revealed excellent biocompatibility, osseointegration and a low affinity for bacterial plaque compared to standard metal implants (titanium implants) [107–109]. The utilization of AM technology is beneficial for the fabrication of zirconia-based ceramic dental implants as they can produce customized geometrics and complex structures. The technology can also improve bioactivity without any surface alterations, such as sandblasting, etching or coating [104]. Nevertheless, it is essential that the functional surface quality of zirconia-based implants fabricated from conventional techniques be enhanced to improve mechanical functions such as wear resistance and fatigue. Moreover, the surface treatments can improve bioactive functions, such as cell proliferation, adhesion, bonding strength, and bacterial decolonization [110].

For example, Osman et al. [111] fabricated 3D printed zirconia implants using DLP technology and evaluated the dimensional accuracy, surface topography, and flexural strength (Table 6). They showed that custom-designed 3D printed implants revealed satisfactory dimensional precision (root mean square error of 0.1 mm), and the flexural strength (943.2 MPa) is equivalent to that of conservative milled zirconia (800–1000 MPa). The roughness of the surface was found to be 1.59  $\mu\text{m}$  and from the SEM analysis, it was observed that the presence of

Applications	Materials	Fabrication techniques	Mechanical properties	Others	Ref.
Dental implants (2017)	YSZ	DLP (from Delta Co.)	Flexural strength 632.1 MPa; Vickers hardness 14.72 GPa	—	[112]
Root analogue implants (RAI) (2017)	YSZ 27 vol%	DLP (from Admatec)	Weibull modulus 3.5; Fracture toughness 6.7 MPa. $\text{m}^{1/2}$	Density 96.9%; Shrinkage 20 vol %	[113]
Dental implants (2017)	YSZ	DLP (from Admatec)	Flexural strength 943 MPa	Dimensional accuracy 0.089 mm and SURFACE roughness 1.59 $\mu\text{m}$	[111]
Medical implants (cube, cuboidal, and bar shaped) (2019)	ATZ 70 wt%	LCM	Flexural strength 430 MPa	Density 5.45 g/cm <sup>3</sup> ; accuracy 70–88%	[114]
Hip implant (2019)	YSZ-ZnO (coating)	FDM and gel casting	—	MC3T3-E1 cells; <i>S. aureus</i> ; <i>E. coli</i> and Rabbit hip joint (4 weeks)	[115]
Dental implants (square shaped) (2021)	Commercial slurry (LithaCon 3Y 230; 3DMix ZrO <sub>2</sub> ; 3D Mix ATZ)	SLA (from 3DCeram and Lithoz GmbH)	Flexural strength 1108.8 MPa (3D Mix ATZ); Weibull modulus 11.1	—	[82]
Dental implants (2021)	ATZ 36–38 vol%	DLP (from Robotfactory)	—	Density 96.8%	[116]

**Table 6.**  
 AM zirconia for implant applications.



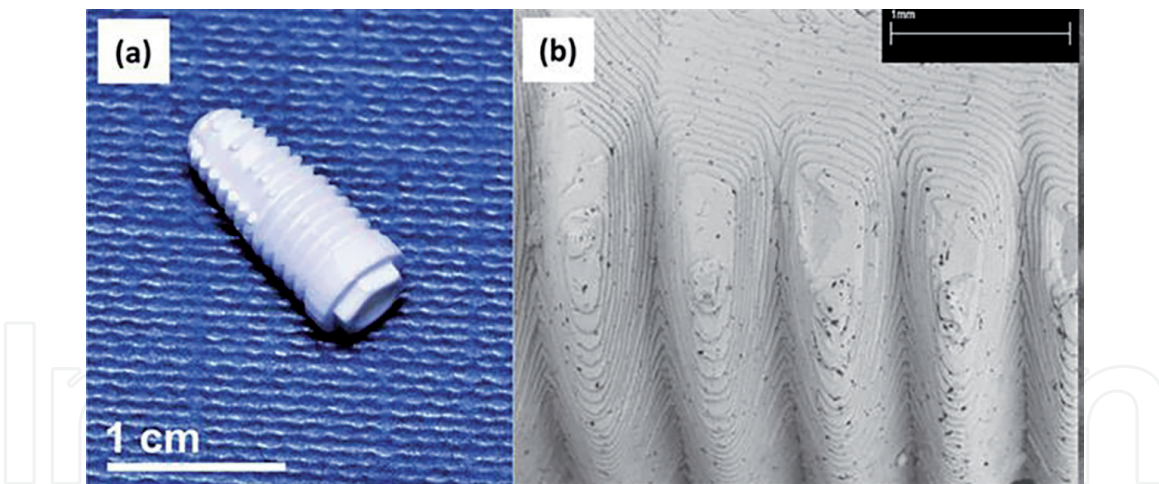


**Figure 4.** Dental implant fabricated using DLP-based additive manufacturing technology. (a) ATZ dental implant-green body, (b) micrograph of the lattice structure [116].

microporosities with interconnected pores (196 nm to 3.3  $\mu\text{m}$ ) and cracks were visible. These flaws were generated during the sintering process or improper dispersion of ceramic particles into the slurry. To enhance the potential microstructure quality of the printed implants, 3D printing parameters need to be optimized.

However, Nakai et al. [82] inspected the microstructure and flexural strength of zirconia-based ceramics formed using SLA (AM technology) and related to CAD/CAM technology (subtractive technology). In their study, the authors compared the commercially available zirconia-based ceramics products. They were two AM 3Y-TZP (LithaCon 3Y 230 and 3D Mix zirconia) products, and one AM ATZ (3DMix ATZ) product, with conventionally fabricated 3Y-TZP (LAVA plus). The experimental outcomes confirmed that the flexural strength and microstructure of AM zirconia are sufficient and close to that of conventionally (subtractive) manufactured zirconia. AM ATZ exhibited higher flexural strength (1108.8 MPa) than 3Y-TZP. Both 3Y-TZP and ATZ are suitable for dental implants. Moreover, variation in the AM process and the impact of building alignment can alter the mechanical properties of AM zirconia. To promote the practical reliability of AM zirconia implants, the relationship between the surface morphology and bioactivity of zirconia needs to be evaluated in a future study. Recently, Magnani et al. [116] presented the potential capability of DLP printing technology to fabricate the dental implants with a new high-performance ATZ composite material (**Figure 4**).

### 3.2 Bone-regeneration applications

The clinical success of zirconia bioceramics in the human environment in the form of dental posts, teeth, and crowns in the dentistry field encouraged biomedical researchers to exploit the biological and mechanical properties of zirconia bioceramics for bone-regeneration applications. Accordingly, developing zirconia-based scaffolds with high precision and dimensional stability is vital to satisfy increasingly challenging requirements for bone-regeneration requests. At present, there is a lack of a simple commercial approach to construct 3D zirconia structures, however, the proposal of AM in 3D zirconia scaffold construction shows great potential. Biomedical engineers targeted AM-based technologies for the zirconia scaffold preparations (**Table 7**). Unlike conventional bioceramics, initial attempts to fabricate zirconia bioceramics were mainly concentrated on multi-pass extrusion techniques [44]. The multi-pass extrusion technique is a simple AM technique in which the ethylene-vinyl acetate polymers were blended with zirconia powders to execute extrusion (the extrusion is repeated to construct the scaffold with constant porous core structure). The extrusion proportion, pore-gradient

Materials	Fabrication techniques	Composite/coating materials and infiltration/intermediate layer	Porosity and pore size	Mechanical properties	Biological properties (in vitro and in vivo)	Ref.
YSZ 48–43 vol% (2011)	Multipass extrusion	Intermediate layer HA ( $\alpha$ -TCP)–YSZ; coating: HA	77% and 86 $\mu\text{m}$	Compression strength: 53 MPa	MG-63 cells	[117]
YSZ (2011)	3D Rapid Prototyper (ABS template) followed by slurry impregnation	Coating: mesoporous bioglass	63–68% and 500–800 $\mu\text{m}$	Compression strength: 44.35–123.32 MPa	SBF and BMSC cells	[118]
YSZ 10 vol% (2011)	Sponge replica and electrospinning	Intermediate layer YSZ-BCP; coating: BCP	67.68–69.65%	Compression strength: 4.83–4.97 MPa	MG-63 cells	[119]
ZrO <sub>2</sub> 50 vol.% (2012)	Free-form	—	40% and 350 $\mu\text{m}$	—	Case study (maxilla)	[120]
YSZ 45–40 vol% (2012)	Multipass extrusion	Intermediate layer: HA-YSZ; coating: HA	—	Compression strength: 7–20 MPa	MG-63 cells	[121]
YSZ 46–41 vol% (2012)	Multipass extrusion	Intermediate layer: YSZ-BCP; coating: PCL/BCP	92–78%	Compression strength: 8.27–12.7 MPa	MG-63 cells	[122]
YSZ 70 wt% (2014)	Direct ink writing (DIW)	—	55 and 63%	Compression strength: 8 and 10 MPa	HCT116 cells	[123]
ZrO <sub>2</sub> -CaSiO <sub>3</sub> (2014)	SLS	Composite: ZrO <sub>2</sub> (10–40 wt%)	70% and 1600 $\mu\text{m}$	Compression strength: 17.9–44.1 MPa; fracture toughness 1.14–1.66 MPa.m <sup>1/2</sup>	SBF and MG-63 cells	[124]
YSZ-PVP (2016)	Electrospinning	—	—	Modulus 1.11 MPa	HMSC cells	[125]
ZrO <sub>2</sub> - $\beta$ -TCP (2016)	3D Rapid Prototyper (ABS template) followed by impregnation	Composite: ZrO <sub>2</sub> (10–50 wt%)	68.5–82.5%	Compression strength: 3–15 MPa; Modulus 184–396 MPa	PBS and MG-63 cells	[126]
ZrO <sub>2</sub> - $\beta$ -TCP (2017)	3D Bioplotter	Composite: ZrO <sub>2</sub> (30 wt%)	60–76.46% and 160–226 $\mu\text{m}$	Compression strength: 7–12.025 MPa	MG-63 cells	[117]
ZrO <sub>2</sub> -PCL 6–30 wt.% (2017)	Electrospinning	—	—	—	3T3 cells	[127]

Materials	Fabrication techniques	Composite/coating materials and infiltration/intermediate layer	Porosity and pore size	Mechanical properties	Biological properties (in vitro and in vivo)	Ref.
YSZ-Al <sub>2</sub> O <sub>3</sub> (ZTA) 70 wt% (35.5 vol%) (2018)	Robocasting	Composite: ZTA (YSZ-16 wt.%)	50% and 245 μm	—	HOB cells	[128]
ZrO <sub>2</sub> -BCP (2018)	FDM	Composite: ZrO <sub>2</sub> (10 wt%)	350 μm	Compression strength: 0.5 MPa	MG-63 and hMSCs cells	[129]
YSZ 48 vol% (2019)	Robocasting	—	200–500 μm	—	—	[130]
ZrO <sub>2</sub> -β- Ca <sub>2</sub> SiO <sub>4</sub> (2019)	3D Bioplotter	Composite: ZrO <sub>2</sub> (5, 10, 15 wt%)	~67%	Compression strength: 3.9–6.1 MPa	SBF and BMSC cells; RAT calvarial defect (8 weeks)	[131]
ZrO <sub>2</sub> -HA 60 wt% (2019)	DLP	Composite: ZrO <sub>2</sub> (1, 3, 6 wt%)	—	Tensile strength (29.4%); bending strength (23.9%)	BMSC cells	[132]
ZrO <sub>2</sub> -PCL (2020)	FDM	Composite: ZrO <sub>2</sub> (5, 10, 20 wt%)	46.2–47% and 459.2–462.7 μm	Compression strength: 5.5–7.9 MPa; Modulus 43–67 MPa	MC3T3-E1 cells	[133]
YSZ (2020)	DLP	Composite: HA (10, 20, 30 wt%)	54.6%	Compression strength: 52.25 MPa; compression strength: after soaking in SBF (25 MPa)	SBF and MC3T3-E1 cells	[134]
YSZ 40 vol% (2020)	FDM and Freeze drying	Intermediate layer: Glass (Infiltration); coating: glass/ Zn-HA (~1 μm) and gelatin/ alginate	40% and 300–450 μm	Compression strength: 68.2– 89.8 MPa; Modulus 1.7–2.6 GPa; Strain energy density 1.8–4.2 MJ/m <sup>3</sup>	DPCs cells	[74]
YSZ 39.5 vol% (2021)	Direct ink writing (DIW)	Intermediate layer: FA; coating: HA (~20 μm)	61.1–75.3%	Compression strength: 20.8–62.9 MPa	SBF	[135]

**Table 7.**  
*AM zirconia for bone tissue regeneration applications.*

rate, and microstructure are the critical parameters in controlling the final output of the zirconia scaffolds. More importantly, to increase the biocompatibility of zirconia binary mixtures ( $ZrO_2/Al_2O_3$ ), fabrication of binary scaffolds with alternating  $ZrO_2$  and  $Al_2O_3$  layers with 3D-interconnected micropores are also demonstrated [136]. However, the multi-pass extrusion designs were not controlled using modern numerical methods. In subsequent years, computerized extrusion-based techniques like 3D Bioplotter and FDM were introduced to precisely design the 3D zirconia scaffolds. Zirconia-based scaffolds ( $\beta-Ca_2SiO_4$ /zirconia scaffolds) fabricated using the 3D-Bioplotter technique were verified to induce bone-regeneration properties in an actual biological atmosphere using a rat model [131]. In FDM, zirconia ceramics are generally blended with polymers such as polycaprolactone to execute a computerized melt mixing process, which can construct a regular grid scaffold [133]. More importantly, biopolymers embedded in zirconia-based scaffolds fabricated using FDM were found to provide additional mechanical support, as well as bioactivity for the zirconia ceramics (Figure 5). Compared to the pristine zirconia-based scaffolds (alginate/gelatine), biopolymer embedded zirconia ceramics were found to exhibit the extracellular matrix (ECM) of the bone tissue, which is essential to imitate the biological environment [74]. Subsequently, considerable research efforts were dedicated to formulating zirconia-based scaffolds using the direct ink writing (DIW) or robocasting method (extrusion-based AM-based technique). 3D zirconia scaffolds fabricated with controlled pore openings and thread dimensions using the DIW method were found to possess high porosity (61% and 75%). More importantly, hydroxyapatite/fluorapatite-based coatings on the DIW derived zirconia-based scaffolds were needed to enhance its bioactivity [135]. Photopolymerization-based AM techniques including DLP and SLS were also studied for the fabrication of zirconia-based scaffolds. Specifically, DLP technology was found to have high accuracy and faster processing ability than other AM-based techniques. The ultraviolet light is irradiated on the zirconia suspensions (prepared by optimizing the solid loading of the zirconia powders, organic monomer, potentiators, and dispersant) to articulate the final design. It is important to perform heat treatment in a high-temperature vacuum furnace to avoid internal cracks and imperfections in the heat-treated zirconia scaffolds [132]. Although SLS-based techniques were widely studied for calcium-based bioceramics, the use of SLS techniques to construct zirconia has been limited due to low zirconia concentration. Mostly, zirconia is blended in minimum volume fraction with other bioactive materials like calcium silicates to avoid the

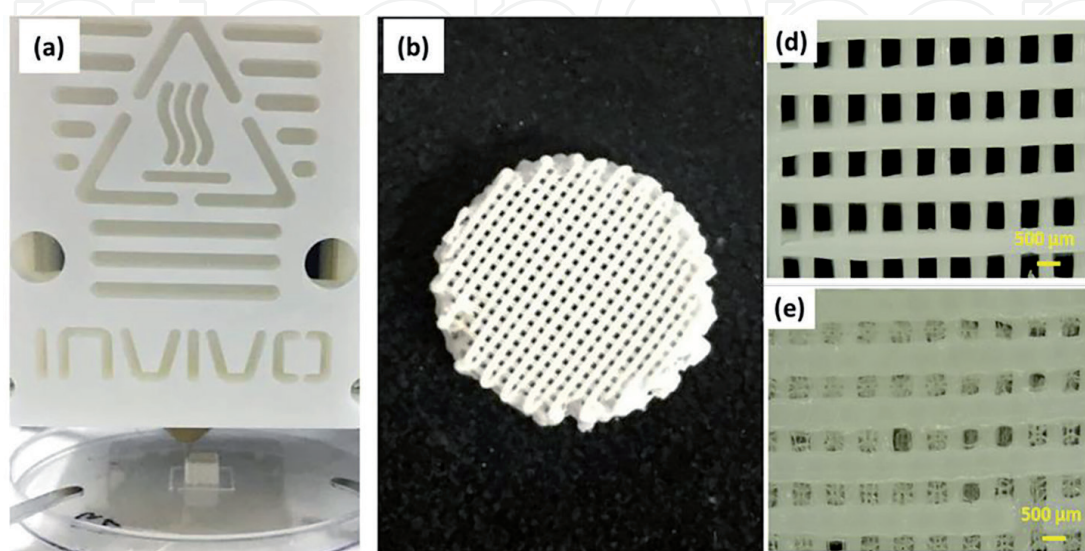


**Figure 5.** (a) Scaffold printing using FDM, (b) digital photograph of the printed zirconia scaffold, (d) microscopic images of zirconia scaffold, and (e) polymer embedded zirconia scaffold [74].

unwanted agglomeration-induced material degradation [124]. In addition, to replicate the nano-to-microscale configuration of the ECM of bone tissue, electrospinning of the zirconia-based scaffolds was experimented with. It is believed that the zirconia scaffolds subjected to electrospinning exhibited high endurance to the inbound load from the bone tissue when compared to conventional more fragile scaffolds [125].

## **4. Outlook and prospective**

Zirconia is a classic bioceramic, and its use in the dental and biomedical fields is inevitable. Hence, extensive research efforts have been dedicated to maximizing the potential of AM technologies to formulate the zirconia ceramics into a precise bone or tooth replacement, scaffolds, implants, and crowns. Though, zirconia scaffolds are directly involved in the human environment (in both dental and biomedical fields), the requirements of each field are evidently different. For instance, the zirconia scaffolds should have adequate porosity for bone-regeneration applications and patient-specific design, whereas, zirconia scaffolds for dental restoration and implants need not have a porous structure; instead, they should retain complex shapes with solid/hollow structures. Hence, the scaffold processing via AM also needs to be precise for each application. AM or 3D printing has revolutionized the designing of complex human hard tissues with an excellent surface finish, minimum material wastage, and high fabrication speed compared to conventional techniques. However, AM also suffers from some inherent limitations and challenges. The primary challenges include difficulties in raw material preparation, process control, and immature designs (**Figure 6**). Research advancements achieved by the metal and polymers-based scaffolds via AM-based techniques both in the laboratory and at clinical levels are far ahead when compared to the practically challenging zirconia-based ceramics due to their inherent challenging properties (brittleness, high melting point, and high density). Hence, it is essential to pinpoint the existing challenges in the research investments and activities that restrict the feasibility of AM-based technologies in fabricating zirconia-based ceramics at the laboratory, clinical, and industrial levels.

### **4.1 Laboratory challenges**

Although different types of AM technologies are available for formulating bioceramics, only a few techniques are effective in the fabrication of zirconia parts with minimal imperfections. Despite the large number of AM technologies suitable for processing ceramics, each technique has its individual advantages and limitations. The primary issue for printing starts from the raw material (feedstock/slurry) preparation itself. For example, in extrusion-based techniques, temperature, pressure, nozzle size, and computer-generated design files (scaffold models) can be fed easily to the computer to accomplish the anticipated requirements. However, poor printability, nozzle blockage, and poor flowability of the feedstock have been major bottlenecks (due to the high density and hardness of zirconia) in designing zirconia-based scaffolds for bone-regeneration applications.

Compared to FDM-based techniques, SLA-based techniques have been extensively explored for the fabrication of zirconia-based ceramics due to the excellent surface finish and precision produced by the technology. Commercial SLA printers are now available for zirconia-based ceramics. However, the uneven distribution and particle aggregation of zirconia particles in the slurry suspension upsetting the light scattering properties (cure depth, curing time, and the energy of the UV light source) is a challenging issue. As a result, geometrical overgrowth is unavoidable due to the high refractive index of the zirconia. (SLA-based techniques are mainly



**Figure 6.**  
*Major challenges of AM zirconia-based ceramics.*

controlled by the light source, refractive index, volume fraction, and particle size.) The most common problem associated with SLA-based techniques for zirconia-based ceramics is the delamination among the layers, which invariably disturbs the physical and mechanical properties of the sintered zirconia parts.

SLS-based techniques, however, can produce scaffolds with high precision, but they are rarely explored for zirconia-based ceramics due to the expensive and complicated control parameters. In particular, the high melting point of zirconia requires pre-heating of the powder bed ( $>1000^{\circ}\text{C}$ ) to avoid cracks caused by the thermal stress induced by the high-power laser source. Nevertheless, SLS-based techniques have represented a single-step scaffolding process for formulating zirconia scaffolds with full density. The requirement and urgency of developing this technique further for zirconia-based scaffolds are debatable.

For all the above, the major disadvantages of AM-based techniques except direct SLS-based techniques are the low-volume fraction of the zirconia in the feedstock ( $<60\%$ , in which the polymer occupies the remaining portion). After debinding of polymers, the printed scaffolds can retain only half of the parent zirconia properties, which invariably affects the expected properties of the final sintered zirconia-based scaffolds.

In general, the strength and life of ceramic materials are directly associated with the type and level of residual stress that developed during the AM process. The major issue of any 3D printing system for the fabrication of zirconia parts is the internal (residual) stress, which is formed either during the printing process or during the post-process. The residual stress generated during the post-process includes high-temperature thermal treatment (sintering process) upon cooling or due to the difference in the thermal expansion coefficient (CTE) between the composite material of zirconia/bilayer material [137]. In other words, the mismatch of the CTE of two different materials can induce residual stress (tensile). Correspondingly, it was demonstrated that the selection of slow cooling and firing program of ceramic can potentially reduce the stress, which will also decrease the risk of chipping of porcelain layer in zirconia dental restoration [138]. Moreover, residual stress has a direct effect on the aging process. For instance, the tensile stresses of the zirconia composite can accelerate the aging

process of the zirconia parts in body fluids [137]. It can be regulated by the stabilizer material nature and content of the zirconia phase in the composite. The most common diagnostic techniques employed for the residual stress measurements include X-ray diffraction, nanoindentation, Raman spectroscopic analysis, thermal tempering using a two-dimensional (2D) analytical model, and three-dimensional (3D) finite element simulation. However, the magnitude of the residual stress of zirconia parts varies from location to location of geometry. Also, the residual stress distribution is affected by the thickness and geometry of the zirconia parts [139]. Upcoming research should be focused on the residual stress of the AM zirconia parts are need to consider.

## **4.2 Clinical challenges**

Although diverse AM-based research studies claim that zirconia-based scaffolds are practicable, true accomplishments are only determined based on the result of the clinical studies. In this regard, there are many unaddressed areas of applications when applying AM-based zirconia to real-world dental and bone restoration that are unresolved. For example, there are internal defects (cracks, porosity) that are formed during layering/printing or postprinting of the designed zirconia prostheses using AM-based techniques. They could affect the mechanical strength of AM zirconia crowns, bridges, implants, and scaffolds and result in a failure to satisfy the dental and biomedical requirements [57]. Nevertheless, optimum porosity is essential to guide cell adhesion or osteointegration. Hence, the stability among the material properties and biological requests need to be established by optimizing the slurry formulation/feedstock and sintering procedures on whatever AM-based techniques are used. The major challenges of 3D printed dental prostheses for real clinical applications are surface finishing/topography, staircase effects, geometrical overgrowth, and mechanical properties. Specifically, the marginal tolerance requirement ( $< 0.1$  mm) for dental prosthetic applications via AM-based techniques is hard to realize, particularly when material strength and density are also mandatory [54, 140].

Uneven shrinkage is caused by the inbound technical shortage of AM-based techniques. Unresolved accuracy in the z-direction compared to the x and y-directions induces densification of ceramic powders within the layer and related issues (degree of polymerization and layer thickness). Overall, the printing parameters along the z-direction are yet to be optimized in such a way that the dimensional accuracy of the zirconia parts is achieved using AM-based techniques capable of addressing the patient-specific requirements. The technical imperfections in design may lead to plaque accumulation, risk of microleakage, and local inflammation [141, 142]. Thus, the relationship between dimensional precision and clinical adoption is critical to the adoption of any AM-based techniques.

Because the scaffolds need to be in direct contact with biological fluids, parts sterilization is important. Hence, biomedical engineers should be aware of the sterilization requirements while designing zirconia-based parts using AM-based techniques. The scaffolds should not lose their characteristic properties even after sterilization. Limited in vivo studies have been devoted to determining the after-effects of zirconia-based scaffolds on the biological environment. These confirm that the AM-based techniques for zirconia-based ceramics are still in infancy. Hence, biomedical engineers should be conscious of the importance of in vivo studies to realizing the practical applications of zirconia-based scaffolds.

## **4.3 Industrial (cost and resource) challenges**

Leading biomedical implant manufacturing companies including Stryker Corp, ZERAMEX, Straumann ceramic, Nobel Biocare, Zimmer Biomet, Wright Medical,

Globus Medical, and Integra Lifesciences focused on developing, manufacturing, and promoting zirconia-based biomedical implants as a material of choice via additive manufacturing technology. Design flexibility, material productivity, and low-volume production feasibility are the prime factors behind the interest in additive manufacturing technology among the leading companies. However, AM-based technologies facing undeniable difficult challenges to fabricate zirconia-based scaffolds. Though adopting AM-based technologies for zirconia implants needs time and determination, the most important challenge lies in the substantial investment on the principal investment cost for the production floor [143]. Investment in the fabrication of zirconia-based biomedical implants from AM-based technologies is not only about equipment cost. It includes the investments in the AM ecosystem as well, which involves material, software, manpower coaching, postprocessing apparatus, documentation, and merging all facilities capable of mass production. More importantly, capital investment and material resources will be added to the above-stated challenges, which is large enough for a corporation to invest in AM as an aggregate. Hence, long-term cost assessment challenges were ahead for any biomedical implant company to unlock the AM-based technology to process zirconia-based scaffolds for wider marketplaces [143].

## 5. Conclusions

New technologies often mean new construction techniques and material and resource applications. AM has become a potentially vital technology in fabricating zirconia-based materials for various critical-sized applications, including bone scaffolds and dental crowns, bridges, and implants. As both AM-based technology and zirconia-based materials are in their infancy for scaffold application, it is essential to create awareness and sensitization among researchers. For example, among the AM-based technology, very few 3D printing systems (SLA, SLS, and DLP) are successful in manufacturing zirconia-based ceramics as scaffolds in the lab scale itself. This is inadequate when compared to well-established 3D printing systems for the use of metal and polymer materials, hence there is a prolonged difficulty in the clinical accomplishment of zirconia-based scaffolds. Though the mechanical properties of the zirconia parts achieved via 3D printing are comparable to the conventional zirconia parts, still some inbound issues such as internal defects (crack and porosities) and dimensional accuracies need to be enhanced. Moreover, for the enhanced bioactivity of zirconia parts, precise selection of the bioactive material and surface treatment strategies (coating/composite) are still under search. It has to be declared here that the essential printing parameters, materials preparation, and the development of the printer capability are progressively taken care of by the biomedical experts in the recent reports. Hence, collective efforts need to be dedicated in collaboration with academia, AM-machine developers, and clinical end-users to share their materials and design requirements to achieve the expected goals. The collective scientific outcomes, together with materials engineering and manufacturing technology, are extremely important in actualizing any emerging technology. AM-based technology could be utilized for manufacturing zirconia-based ceramics, which would be a milestone for society if all its current limitations can be systematically and creatively addressed.

## Acknowledgements

This work was supported by the National Research Foundation of Korea (NRF). Grant funded by the Korean government (MSIT) (No. 2019R1A2C108945613).



## Conflict of interest

The authors declare no conflict of interest.

## Notes/thanks/other declarations

We thank Pavithra Kumaresan, Karthik Narayanan, and Hariprasath Sekar for their timely help during editing the manuscript.

## Abbreviations

Y-TZP (or) YSZ	yttrium tetragonal zirconia polycrystal (or) yttria stabilised zirconia
ZTA	zirconia toughened alumina
Mg-PSZ (or) MgSZ	magnesia partially stabilized zirconia (or) magnesium stabilized zirconia
Y <sub>2</sub> O <sub>3</sub>	yttrium oxide
ZrO <sub>2</sub>	zirconium dioxide/zirconia
Al <sub>2</sub> O <sub>3</sub>	aluminium oxide/alumina
MgO	magnesium oxide
ATZ	alumina toughened zirconia
ZnO	zinc oxide
HA	hydroxyapatite
TCP	tricalcium phosphate
BCP	bicalcium phosphate
FA	fluoroapatite
CaP	calcium phosphate
PMMA	polymethacrylate
PCL	polycaprolactone
CS	chitosan
SF	silk fibrin
POM	polyoxometalates
PLA	polylactic acid
PRP	plasma rich protein
HS	heparin sulfate
CZ	calcium zirconate
Ca <sub>2</sub> SiO <sub>4</sub>	calcium silicate
PVP	polyvinylpyrrolidone
ABS	acrylonitrile butadiene styrene
Zn-HA	zinc doped hydroxyapatite
DIW	direct ink writing
BJ	binder jetting
FDM	fused deposition modelling
DLP	digital light processing
CAD/CAM	computer aided design/computer aided milling
SLS	selective laser sintering
SLM	selective laser melting
<i>S. aureus</i>	<i>Streptococcus aureus</i>
<i>E. coli</i>	<i>Escherichia coli</i>
HOS	human osteosarcoma
SBF	stimulated body fluid

MG63	osteosarcoma cells
MCT3-E1	murine preosteoblast cells
BMSC	bone marrow-derived mesenchymal stem cells
L929	murine fibroblast cells
PBS	phosphate buffered saline
HGF	human gingival fibroblast cells
OB6	murine bone marrow-derived osteoblastic cells
HCT116	human colon carcinoma cells
HOB	human osteoblast cells
hMSC	human mesenchymal stem cells
DPCs	dental pulp cells

## Author details

Sakthiabirami Kumaresan<sup>1,2</sup>, Soundharrajan Vaiyapuri<sup>3</sup>, Jin-Ho Kang<sup>1</sup>,  
Nileshkumar Dubey<sup>4</sup>, Geetha Manivasagam<sup>5</sup>, Kwi-Dug Yun<sup>1</sup> and Sang-Won Park<sup>1,6\*</sup>

1 Department of Prosthodontics, Dental Science Research Institute, School of Dentistry, Chonnam National University, Gwangju, Republic of Korea

2 Chonnam National University Biomedical Evaluation and Research Center, Gwangju, Republic of Korea

3 Department of Materials Science and Engineering, Chonnam National University, Gwangju, Republic of Korea

4 Faculty of Dentistry, National University of Singapore, Singapore

5 Centre for Biomaterials, Cellular and Molecular Theranostics, School of Mechanical Engineering, Vellore Institute of Technology (VIT), Vellore, Tamil Nadu, India

6 RIS Advanced Center for Biomaterials, School of Dentistry, Chonnam National University, Gwangju, Republic of Korea

\*Address all correspondence to: [psw320@chonnam.ac.kr](mailto:psw320@chonnam.ac.kr)

## IntechOpen

© 2022 The Author(s). Licensee IntechOpen. This chapter is distributed under the terms of the Creative Commons Attribution License (<http://creativecommons.org/licenses/by/3.0>), which permits unrestricted use, distribution, and reproduction in any medium, provided the original work is properly cited. 

## References

- [1] Ivanova N, Gugleva V, Dobрева M, Pehlivanov I, Stefanov S, Andonova V. We are IntechOpen, the world's leading publisher of Open Access books Built by scientists, for scientists TOP 1%. INTECH. 2016;**i**(tourism):13
- [2] Dubey N, Ferreira JA, Malda J, Bhaduri SB, Bottino MC. Extracellular matrix/amorphous magnesium phosphate bioink for 3D bioprinting of craniomaxillofacial bone tissue. *ACS Applied Materials & Interfaces*. 2020;**12**(21):23752-23763. Available from: <https://pubmed.ncbi.nlm.nih.gov/32352748>
- [3] Saravanan S, Vimalraj S, Thanikaivelan P, Banudevi S, Manivasagam G. A review on injectable chitosan/beta glycerophosphate hydrogels for bone tissue regeneration. *International Journal of Biological Macromolecules*. 2019;**121**:38-54. Available from: <https://www.sciencedirect.com/science/article/pii/S0141813018331829>
- [4] Best SM, Porter AE, Thian ES, Huang J. Bioceramics: Past, present and for the future. *Journal of the European Ceramic Society*. 2008;**28**(7):1319-1327. Available from: <https://www.sciencedirect.com/science/article/pii/S0955221907005961>
- [5] Christel P, Meunier A, Dorlot JM, Crolet JM, Witvoet J, Sedel L, et al. Biomechanical compatibility and design of ceramic implants for orthopedic surgery. *Annals of the New York Academy of Sciences*. 1988;**523**:234-256
- [6] Tosiriwatanapong T, Singhatanadgit W. Zirconia-based biomaterials for hard tissue reconstruction. *Bone Tissue Regen Insights*. 2018;**9**:1179061X18767886. DOI: 10.1177/1179061X18767886
- [7] Manicone PF, Rossi Iommetti P, Raffaelli L. An overview of zirconia ceramics: Basic properties and clinical applications. *Journal of Dentistry*. 2007;**35**(11):819-826
- [8] Piconi C, Maccauro G. Zirconia as a ceramic biomaterial. *Biomaterials*. 1999;**20**:1-25
- [9] Saridag S, Tak O, Alniacik G. Basic properties and types of zirconia: An overview. *World Journal of Stomatology*. 2013;**2**(3):40-47
- [10] Sakthiabirami K, Soundharrajan V, Kang J-H, Yang YP, Park S-W. Three-dimensional zirconia-based scaffolds for load-bearing bone-regeneration applications: Prospects and challenges. *Materials (Basel)*. 2021;**14**(12). Available from: <https://www.mdpi.com/1996-1944/14/12/3207>
- [11] Heuer AH, Lange FF, Swain MV, Evans AG. Transformation toughening: An overview. *Journal of the American Ceramic Society*. 1986;**69**(3):i-iv. DOI: 10.1111/j.1151-2916.1986.tb07400.x
- [12] Kelly JR, Denry I. Stabilized zirconia as a structural ceramic: An overview. *Dental Materials*. 2008;**24**(3):289-298
- [13] Ganapathy P, Manivasagam G, Rajamanickam A, Natarajan A. Wear studies on plasma-sprayed Al<sub>2</sub>O<sub>3</sub> and 8mol% of Yttrium-stabilized ZrO<sub>2</sub> composite coating on biomedical Ti-6Al-4V alloy for orthopedic joint application. *International Journal of Nanomedicine*. 2015;**10**(Suppl 1):213-222. Available from: <https://pubmed.ncbi.nlm.nih.gov/26491323>
- [14] Denry I, Kelly JR. Emerging ceramic-based materials for dentistry. *Journal of Dental Research*. 2014;**93**(12):1235-1242
- [15] Volpato CAM, Garbelotto LGD, Fredel MC, Bondioli F. Application of zirconia in dentistry: Biological,

mechanical and optical considerations. In: *Advances in Ceramics—Electric and Magnetic Ceramics, Bioceramics, Ceramics and Environment*. 2011. Available from: <https://www.intechopen.com/chapters/18282>

[16] Chen Y-W, Moussi J, Drury JL, Wataha JC. Zirconia in biomedical applications. *Expert Review of Medical Devices*. 2016;**13**(10):945-963. DOI: 10.1080/17434440.2016.1230017

[17] Gadow R, Kern F. Pressureless sintering of injection molded zirconia toughened alumina nanocomposites. *Journal of the Ceramic Society of Japan*. 2006;**114**(1335):958-962

[18] Wang S, Yu JY, Li Q, Zheng EY, Duan YG, Qi G. Preparation of gradient ZTA ceramic by centrifugal slip casting method. *Advances in Materials Research*. 2012;**569**:324-327

[19] Gautam C, Joyner J, Gautam A, Rao J, Vajtai R. Zirconia based dental ceramics: Structure, mechanical properties, biocompatibility and applications. *Dalton Transactions*. 2016;**45**(48):19194-19215

[20] He Q, Jiang J, Yang X, Zhang L, Zhou Z, Zhong Y, et al. Additive manufacturing of dense zirconia ceramics by fused deposition modeling via screw extrusion. *Journal of the European Ceramic Society*. 2021;**41**(1): 1033-1040. Available from: <https://www.sciencedirect.com/science/article/pii/S0955221920307421>

[21] Ferrage L, Bertrand G, Lenormand P, Grossin D, Ben-Nissan B. A review of the additive manufacturing (3DP) of bioceramics: Alumina, zirconia (PSZ) and hydroxyapatite. *Journal of the Australian Ceramic Society*. 2017;**53**(1):11-20. DOI: 10.1007/s41779-016-0003-9

[22] Aytac Z, Dubey N, Daghery A, Ferreira JA, de Souza Araújo IJ,

Castilho M, et al. Innovations in craniofacial bone and periodontal tissue engineering—From electrospinning to converged biofabrication. *International Materials Review*. 2021;**0**(0):1-38. DOI: 10.1080/09506608.2021.1946236

[23] Kang J-H, Jang K-J, Sakthiabirami K, Oh G-J, Jang J-G, Park C, et al. Fabrication and characterization of 45S5 bioactive glass/thermoplastic composite scaffold by ceramic injection printer. *Journal of Nanoscience and Nanotechnology*. 2020;**20**(9):5520-5524

[24] Zhang X, Wu X, Shi J. Additive manufacturing of zirconia ceramics: A state-of-the-art review. *Journal of Materials Research and Technology*. 2020;**9**(4):9029-9048. Available from: <https://www.sciencedirect.com/science/article/pii/S2238785420313958>

[25] Galante R, Figueiredo-Pina CG, Serro AP. Additive manufacturing of ceramics for dental applications: A review. *Dental Materials*. 2019;**35**(6):825-846. Available from: <https://www.sciencedirect.com/science/article/pii/S0109564118304263>

[26] Singh S, Ramakrishna S. Biomedical applications of additive manufacturing: Present and future. *Current Opinion in Biomedical Engineering*. 2017;**2**:105-115. Available from: <https://www.sciencedirect.com/science/article/pii/S2468451117300296>

[27] Halloran JW. Freeform fabrication of ceramics. *British Ceramic Transactions*. 1999;**98**(6):299-303

[28] Deckers J, Vleugels J, Kruth JP. Additive manufacturing of ceramics: A review. *Journal of Ceramic Science and Technology*. 2014;**5**(4):245-260

[29] Sun J, Chen X, Wade-Zhu J, Binner J, Bai J. A comprehensive study of dense zirconia components fabricated by additive manufacturing. *Additive Manufacturing*. 2021;**43**:101994.

Available from: <https://www.sciencedirect.com/science/article/pii/S2214860421001597>

[30] Li W, Ghazanfari A, McMillen D, Leu MC, Hilmas GE, Watts J. Characterization of zirconia specimens fabricated by ceramic on-demand extrusion. *Ceramics International*. 2018;**44**(11):12245-12252. Available from: <https://www.sciencedirect.com/science/article/pii/S0272884218308630>

[31] Shishkovsky I, Sherbakov V, Ibatullin I, Volchkov V, Volova L. Nano-size ceramic reinforced 3D biopolymer scaffolds: Tribomechanical testing and stem cell activity. *Composite Structures*. 2018;**202**:651-659. Available from: <https://www.sciencedirect.com/science/article/pii/S026382231734374X>

[32] Shishkovsky I, Scherbakov V, Volchkov V, Volova L. Laser-assisted nanoceramics reinforced polymer scaffolds for tissue engineering: Additional heating and stem cells behavior. In: *SPIE BiOS Photonics west Proceeding, Dynamics and Fluctuations in Biomedical Photonics XV*. 2018;**10493**:104931T. Available from: <https://lens.org/083-875-320-932-820>

[33] Shishkovsky I, Nagulin K, Sherbakov V. Study of biocompatible nano oxide ceramics, interstitial in polymer matrix during laser-assisted sintering. *International Journal of Advanced Manufacturing Technology*. 2015;**78**(1-4):449-455. DOI: 10.1007/s00170-014-6633-6

[34] Grossin D, Montón A, Navarrete-Segado P, Özmen E, Urruth G, Maury F, et al. A review of additive manufacturing of ceramics by powder bed selective laser processing (sintering/melting): Calcium phosphate, silicon carbide, zirconia, alumina, and their composites. *Open Ceramics*. 2021;**5**:100073. Available from: <https://www.sciencedirect.com/science/article/pii/S2666539521000195>

[35] Bertrand P, Bayle F, Combe C, Goeuriot P, Smurov I. Ceramic components manufacturing by selective laser sintering. *Applied Surface Science*. 2007;**254**(4):989-992. Available from: <https://www.sciencedirect.com/science/article/pii/S0169433207012603>

[36] Shishkovsky IV, Volchkov SE. Ceramics-filled 3D porous biopolymer matrices for tissue-engineering on the stem cell culture: Benchmark testing. In: Bartolo et al., editors. *High Value Manufacturing: Advanced Research in Virtual and Rapid Prototyping*. Taylor & Francis Group; 2014. pp. 121-126. ISBN: 978-1-138-00137-7

[37] Shishkovsky I, Scherbakov V. Selective laser sintering of biopolymers with micro and nano ceramic additives for medicine. *Physics Procedia*. 2012;**39**:491-499. Open access

[38] Shishkovsky I, Yadroitsev I, Bertrand P, Smurov I. Alumina-zirconium ceramics synthesis by selective laser sintering/melting. *Applied Surface Science*. 2007;**254**(4):966-970. Available from: <https://www.sciencedirect.com/science/article/pii/S0169433207012718>

[39] Lee B-T, Kim K-H, Han J-K. Microstructures and material properties of fibrous  $\text{Al}_2\text{O}_3-(m\text{-ZrO}_2)/t\text{-ZrO}_2$  composites fabricated by a fibrous monolithic process. *Journal of Materials Research*. 2004;**19**(11):3234-3241. Available from: <https://www.cambridge.org/core/article/microstructures-and-material-properties-of-fibrous-al2o3mzro2tzro2-composites-fabricated-by-a-fibrous-monolithic-process/F489F154FC488B84FCA0607897D22B75>

[40] Liu Q, Danlos Y, Song B, Zhang B, Yin S, Liao H. Effect of high-temperature preheating on the selective laser melting of yttria-stabilized zirconia ceramic. *Journal of Materials Processing Technology*. 2015;**222**:61-74. Available from: <https://www.>

[sciencedirect.com/science/article/pii/S0924013615000862](https://www.sciencedirect.com/science/article/pii/S0924013615000862)

[41] Verga F, Borlaf M, Conti L, Florio K, Vetterli M, Graule T, et al. Laser-based powder bed fusion of alumina toughened zirconia. *Additive Manufacturing*. 2020;**31**:100959. Available from: <https://www.sciencedirect.com/science/article/pii/S2214860419307870>

[42] Shahzad K, Deckers J, Zhang Z, Kruth J-P, Vleugels J. Additive manufacturing of zirconia parts by indirect selective laser sintering. *Journal of the European Ceramic Society*. 2014;**34**(1):81-89. Available from: <https://www.sciencedirect.com/science/article/pii/S0955221913003531>

[43] Shi Y, Liu K, Li C, Wei Q, Liu J, Xia S. Additive manufacturing of zirconia parts via selective laser sintering combined with cold isostatic pressing. *Check Jixie Gongcheng Xuebao/Chinese Journal of Mechanical Engineering*. 2014;**50**(21):118-123

[44] Chen F, Wu J-M, Wu H-Q, Chen Y, Li C-H, Shi Y-S. Microstructure and mechanical properties of 3Y-TZP dental ceramics fabricated by selective laser sintering combined with cold isostatic pressing. *International Journal of Lightweight Materials and Manufacture*. 2018;**1**(4):239-245. Available from: <https://www.sciencedirect.com/science/article/pii/S2588840418300465>

[45] Wilkes J, Hagedorn Y, Meiners W, Wissenbach K. Additive manufacturing of ZrO<sub>2</sub>-Al<sub>2</sub>O<sub>3</sub> ceramic components by selective laser melting. *Rapid Prototyping Journal*. 2013;**19**(1):51-57. DOI: 10.1108/13552541311292736

[46] Ferrage L, Bertrand G, Lenormand P. Dense yttria-stabilized zirconia obtained by direct selective laser sintering. *Additive Manufacturing*. 2018;**21**:472-478. Available from: <https://www.sciencedirect.com/science/article/pii/S2214860417305602>

[47] Koopmann J, Voigt J, Niendorf T. Additive manufacturing of a steel-ceramic multi-material by selective laser melting. *Metallurgical and Materials Transactions B*. 2019;**50**(2):1042-1051. DOI: 10.1007/s11663-019-01523-1

[48] Huang S, Ye C, Zhao H, Fan Z, Wei Q. Binder jetting yttria stabilised zirconia ceramic with inorganic colloid as a binder. *Advances in Applied Ceramics*. 2019;**118**(8):458-465. DOI: 10.1080/17436753.2019.1666593

[49] Tarafder S, Balla VK, Davies NM, Bandyopadhyay A, Bose S. Microwave-sintered 3D printed tricalcium phosphate scaffolds for bone tissue engineering. *Journal of Tissue Engineering and Regenerative Medicine*. 2013;**7**(8):631-641

[50] Vorndran E, Klarner M, Klammert U, Grover LM, Patel S, Barralet JE, et al. 3D powder printing of  $\beta$ -tricalcium phosphate ceramics using different strategies. *Advanced Engineering Materials*. 2008;**10**(12):67-71

[51] Zhao H, Ye C, Fan Z, Shi Y. 3D Printing of ZrO<sub>2</sub> Ceramic using Nano-zirconia Suspension as a Binder. 2016; (*Icsmim 2015*):654-7

[52] Kang J-H, Jang K-J, Sakthiabirami K, Oh G-J, Jang J-G, Park C, et al. Mechanical properties and optical evaluation of scaffolds produced from 45S5 bioactive glass suspensions via stereolithography. *Ceramics International*. 2020;**46**(2):2481-2488. Available from: <https://www.sciencedirect.com/science/article/pii/S0272884219327798>

[53] Zakeri S, Vippola M, Levänen E. A comprehensive review of the photopolymerization of ceramic resins used in stereolithography. *Additive Manufacturing*. 2020;**35**:101177. Available from: <https://www.sciencedirect.com/science/article/pii/S2214860420305492>

- [54] Dehurtevent M, Robberecht L, Hornez J-C, Thuault A, Deveaux E, Béhin P. Stereolithography: A new method for processing dental ceramics by additive computer-aided manufacturing. *Dental Materials*. 2017;**33**(5):477-485
- [55] Zhang K, He R, Xie C, Wang G, Ding G, Wang M, et al. Photosensitive ZrO<sub>2</sub> suspensions for stereolithography. *Ceramics International*. 2019;**45**(9):12189-12195. Available from: <http://www.sciencedirect.com/science/article/pii/S0272884219306625>
- [56] Jang K-J, Kang J-H, Fisher JG, Park S-W. Effect of the volume fraction of zirconia suspensions on the microstructure and physical properties of products produced by additive manufacturing. *Dental Materials*. 2019;**35**(5):e97-e106. Available from: <https://www.sciencedirect.com/science/article/pii/S0109564118312119>
- [57] Lian Q, Sui W, Wu X, Yang F, Yang S. Additive manufacturing of ZrO<sub>2</sub> ceramic dental bridges by stereolithography. *Rapid Prototyping Journal*. 2018;**24**(1):114-119. DOI: 10.1108/RPJ-09-2016-0144
- [58] He R, Liu W, Wu Z, An D, Huang M, Wu H, et al. Fabrication of complex-shaped zirconia ceramic parts via a DLP-stereolithography-based 3D printing method. *Ceramics International*. 2018;**44**(3):3412-3416. Available from: <https://www.sciencedirect.com/science/article/pii/S0272884217325932>
- [59] Sun J, Binner J, Bai J. 3D printing of zirconia via digital light processing: Optimization of slurry and debinding process. *Journal of the European Ceramic Society*. 2020;**40**(15):5837-5844. Available from: <https://www.sciencedirect.com/science/article/pii/S0955221920304465>
- [60] Khudyakov IV. Fast photopolymerization of acrylate coatings: Achievements and problems. *Progress in Organic Coatings*. 2018;**121**:151-159. Available from: <https://www.sciencedirect.com/science/article/pii/S0300944017310329>
- [61] DiSanto P. Book reviews. *Journal of Transplant Coordination*. 1996;**6**(4):219-220
- [62] Allen NS. Photoinitiators for UV and visible curing of coatings: Mechanisms and properties. *Journal of Photochemistry and Photobiology A: Chemistry*. 1996;**100**(1):101-107. Available from: <https://www.sciencedirect.com/science/article/pii/S1010603096044267>
- [63] Allonas X. Photopolymerization, cationic. *Encyclopedia of Polymer Science and Technology*. 2019:1-30
- [64] Eren TN, Okte N, Morlet-Savary F, Fouassier JP, Lalevee J, Avci D. One-component thioxanthone-based polymeric photoinitiators. *Journal of Polymer Science, Part A: Polymer Chemistry*. 2016;**54**(20):3370-3378
- [65] Hafkamp T, van Baars G, de Jager B, Etman P. A feasibility study on process monitoring and control in vat photopolymerization of ceramics. *Mechatronics*. 2018;**56**:220-241. Available from: <https://www.sciencedirect.com/science/article/pii/S095741581830028X>
- [66] Bae CJ, Ramachandran A, Chung K, Park S. Ceramic stereolithography: Additive manufacturing for 3D complex ceramic structures. *Journal of the Korean Ceramic Society*. 2017;**54**(6):470-477
- [67] McNulty TF, Mohammadi F, Bandyopadhyay A, Shanefield DJ, Danforth SC, Safari A. Development of a binder formulation for fused deposition of ceramics. *Rapid Prototyping Journal*. 1998;**4**(4):144-150. DOI: 10.1108/13552549810239012

- [68] Gonzalez-Gutierrez J, Cano S, Schuschnigg S, Kukla C, Sapkota J, Holzer C. Additive manufacturing of metallic and ceramic components by the material extrusion of highly-filled polymers: A review and future perspectives. *Materials (Basel)*. 2018;**11**(5):2-36. Available from: <https://www.mdpi.com/1996-1944/11/5/840>
- [69] Venkataraman N, Rangarajan S, Matthewson MJ, Harper B, Safari A, Danforth SC, et al. Feedstock material property-process relationships in fused deposition of ceramics (FDC). *Rapid Prototyping Journal*. 2000;**6**(4):244-253. DOI: 10.1108/13552540010373344
- [70] Spoerk M, Gonzalez-Gutierrez J, Sapkota J, Schuschnigg S, Holzer C. Effect of the printing bed temperature on the adhesion of parts produced by fused filament fabrication. *Plastics, Rubber and Composites*. 2018;**47**(1):17-24
- [71] Carneiro OS, Silva AF, Gomes R. Fused deposition modeling with polypropylene. *Materials and Design*. 2015;**83**:768-776. Available from: <https://www.sciencedirect.com/science/article/pii/S0264127515004037>
- [72] Khaliq MH, Gomes R, Fernandes C, Nóbrega J, Carneiro OS, Ferrás LL. On the use of high viscosity polymers in the fused filament fabrication process. *Rapid Prototyping Journal*. 2017;**23**(4):727-735. DOI: 10.1108/RPJ-02-2016-0027
- [73] Banerjee S, Joens CJ. 7—Debinding and sintering of metal injection molding (MIM) components. In: Heaney DF, editor. *Handbook of Metal Injection Molding*, Woodhead Publishing Series in Metals and Surface Engineering. Woodhead Publishing; 2012. pp. 133-180. Available from: <https://www.sciencedirect.com/science/article/pii/B9780857090669500078>
- [74] Sakthiabirami K, Kang J-H, Jang J-G, Soundharajan V, Lim H-P, Yun K-D, et al. Hybrid porous zirconia scaffolds fabricated using additive manufacturing for bone tissue engineering applications. *Materials Science and Engineering: C*. 2021;**123**:111950. Available from: <https://www.sciencedirect.com/science/article/pii/S0928493121000898>
- [75] Cano S, Gonzalez-Gutierrez J, Sapkota J, Spoerk M, Arbeiter F, Schuschnigg S, et al. Additive manufacturing of zirconia parts by fused filament fabrication and solvent debinding: Selection of binder formulation. *Additive Manufacturing*. 2019;**26**:117-128. Available from: <https://www.sciencedirect.com/science/article/pii/S2214860418309904>
- [76] Gaddam A, Brazete DS, Neto AS, Nan B, Ferreira JMF. Three-dimensional printing of zirconia scaffolds for load bearing applications: Study of the optimal fabrication conditions. *Journal of the American Ceramic Society*. 2021;**104**(9):4368-4380. Available from: <https://ceramics.onlinelibrary.wiley.com/doi/abs/10.1111/jace.17874>
- [77] Shao H, Zhao D, Lin T, He J, Wu J. 3D gel-printing of zirconia ceramic parts. *Ceramics International*. 2017;**43**(16):13938-13942
- [78] Yu T, Zhang Z, Liu Q, Kuliiev R, Orlovskaya N, Wu D. Extrusion-based additive manufacturing of yttria-partially-stabilized zirconia ceramics. *Ceramics International*. 2020;**46**(4): 5020-5027. Available from: <https://www.sciencedirect.com/science/article/pii/S0272884219331190>
- [79] Grech J, Antunes E. Zirconia in dental prosthetics: A literature review. *Journal of Materials Research and Technology*. 2019;**8**(5):4956-4964. Available from: <https://www.sciencedirect.com/science/article/pii/S2238785419300419>
- [80] Strub JR, Rekow ED, Witkowski S. Computer-aided design and fabrication



of dental restorations: Current systems and future possibilities. *Journal of the American Dental Association* (1939). 2006;**137**(9):1289-1296

[81] Denry I, Kelly JR. State of the art of zirconia for dental applications. *Dental Materials*. 2008;**24**(3):299-307

[82] Nakai H, Inokoshi M, Nozaki K, Komatsu K, Kamijo S, Liu H, et al. Additively manufactured zirconia for dental applications. *Materials (Basel)*. 2021;**14**(13):3694

[83] Rosenblum MA, Schulman A. A review of all-ceramic restorations. *Journal of the American Dental Association* (1939). 1997;**128**(3):297-307

[84] Darmawan BA, Fisher JG, Trung DT, Sakthiabirami K, Park S-W. Two-step sintering of partially stabilized zirconia for applications in ceramic crowns. *Materials (Basel)*. 2020;**13**(8):1857. Available from: <https://www.mdpi.com/1996-1944/13/8/1857>

[85] Guazzato M, Albakry M, Ringer SP, Swain MV. Strength, fracture toughness and microstructure of a selection of all-ceramic materials. Part II. Zirconia-based dental ceramics. *Dental Materials*. 2004;**20**(5):449-456

[86] Heintze SD, Rousson V. Survival of zirconia- and metal-supported fixed dental prostheses: A systematic review. *The International Journal of Prosthodontics*. 2010;**23**(6):493-502

[87] Beuer F, Stimmelmayer M, Gernet W, Edelhoff D, Güth J-F, Naumann M. Prospective study of zirconia-based restorations: 3-year clinical results. *Quintessence International*. 2010;**41**(8):631-637

[88] Fischer J, Stawarczyk B, Hämmerle CHF. Flexural strength of veneering ceramics for zirconia. *Journal of Dentistry*. 2008;**36**(5):316-321

[89] Schweiger J, Bomze D, Schwentenwein M. 3D printing of zirconia—What is the future? *Current Oral Health Reports*. 2019;**6**(4):339-343. DOI: 10.1007/s40496-019-00243-4

[90] Ebert J, Ozkol E, Zeichner A, Uibel K, Weiss O, Koops U, et al. Direct inkjet printing of dental prostheses made of zirconia. *Journal of Dental Research*. 2009;**88**(7):673-676

[91] Özkol E, Zhang W, Ebert J, Telle R. Potentials of the “Direct inkjet printing” method for manufacturing 3Y-TZP based dental restorations. *Journal of the European Ceramic Society*. 2012;**32**(10):2193-2201. Available from: <https://www.sciencedirect.com/science/article/pii/S0955221912001380>

[92] Silva NRFA, Witek L, Coelho PG, Thompson VP, Rekow ED, Smay J. Additive CAD/CAM process for dental prostheses. *Journal of Prosthodontics*. 2011;**20**(2):93-96. Available from: <https://onlinelibrary.wiley.com/doi/abs/10.1111/j.1532-849X.2010.00623.x>

[93] Liu K, Zhang K, Bourell DL, Chen F, Sun H, Shi Y, et al. Gelcasting of zirconia-based all-ceramic teeth combined with stereolithography. *Ceramics International*. 2018;**44**(17):21556-21563. Available from: <https://www.sciencedirect.com/science/article/pii/S0272884218322958>

[94] Wang W, Yu H, Liu Y, Jiang X, Gao B. Trueness analysis of zirconia crowns fabricated with 3-dimensional printing. *The Journal of Prosthetic Dentistry*. 2019;**121**(2):285-291

[95] Li R, Wang Y, Hu M, Wang Y, Xv Y, Liu Y, et al. Strength and adaptation of stereolithography-fabricated zirconia dental crowns: An in vitro study. *The International Journal of Prosthodontics*. 2019;**32**(5):439-443

[96] Zandinejad A, Revilla-león M, Methani MM, Khanlar LN. The Fracture

Resistance of Additively Manufactured Monolithic Zirconia vs . Bi-Layered Alumina Toughened Zirconia Crowns when Cemented to Zirconia Abutments. Evaluating the Potential of 3D Printing of Ceramic Crowns: An In Vitro Study. *Dentistry Journal*. 2021;**9**(10):115

[97] Revilla-León M, Methani MM, Morton D, Zandinejad A. Internal and marginal discrepancies associated with stereolithography (SLA) additively manufactured zirconia crowns. *The Journal of Prosthetic Dentistry*. 2020;**124**(6):730-737. Available from: <https://www.sciencedirect.com/science/article/pii/S0022391319306109>

[98] Ioannidis A, Bomze D, Hämmerle CHF, Hüsler J, Birrer O, Mühlemann S. Load-bearing capacity of CAD/CAM 3D-printed zirconia, CAD/CAM milled zirconia, and heat-pressed lithium disilicate ultra-thin occlusal veneers on molars. *Dental Materials*. 2020;**36**(4):e109-e116. Available from: <https://www.sciencedirect.com/science/article/pii/S0109564120300166>

[99] Shi Y, Wang W. 3D inkjet printing of the zirconia ceramic implanted teeth. *Materials Letters*. 2020;**261**:127131. Available from: <https://www.sciencedirect.com/science/article/pii/S0167577X1931763X>

[100] Wang W, Sun J. Dimensional accuracy and clinical adaptation of ceramic crowns fabricated with the stereolithography technique. *The Journal of Prosthetic Dentistry*. 2021;**125**(4):657-663. Available from: <https://www.sciencedirect.com/science/article/pii/S0022391320302134>

[101] Li R, Chen H, Wang Y, Sun Y. Performance of stereolithography and milling in fabricating monolithic zirconia crowns with different finish line designs. *Journal of the Mechanical Behavior of Biomedical Materials*. 2021;**115**:104255. Available from: <https://www.sciencedirect.com/science/article/pii/S1751616120307931>

[www.sciencedirect.com/science/article/pii/S1751616120307931](https://www.sciencedirect.com/science/article/pii/S1751616120307931)

[102] Revilla-León M, Al-Haj Husain N, Ceballos L, Özcan M. Flexural strength and Weibull characteristics of stereolithography additive manufactured versus milled zirconia. *The Journal of Prosthetic Dentistry*. 2021;**125**(4):685-690. Available from: <https://www.sciencedirect.com/science/article/pii/S0022391320300871>

[103] Revilla-León M, Mostafavi D, Methani MM, Zandinejad A. Manufacturing accuracy and volumetric changes of stereolithography additively manufactured zirconia with different porosities. *Journal of Prosthetic Dentistry*. 2021. Available from: <https://www.sciencedirect.com/science/article/pii/S0022391320305047>

[104] Osman RB, Swain MV. A critical review of dental implant materials with an emphasis on titanium versus zirconia. *Materials (Basel)*. 2015;**8**(3):932-958

[105] Abd El-Ghany OS, Sherief AH. Zirconia based ceramics, some clinical and biological aspects: Review. *Future Dental Journal*. 2016;**2**(2):55-64. Available from: <http://www.sciencedirect.com/science/article/pii/S2314718016300398>

[106] Van der Zel J. Zirconia Ceramic in Dental CAD/CAM: How CAD/CAM Technology Enables Zirconia to Replace Metal in Restorative Dentistry. *Journal of Dental Technology*. 2007;**2**:17-24

[107] Depprich R, Zipprich H, Ommerborn M, Mahn E, Lammers L, Handschel J, et al. Osseointegration of zirconia implants: An SEM observation of the bone-implant interface. *Head & Face Medicine*. 2008;**4**:25

[108] Schultze-Mosgau S, Schliephake H, Radespiel-Tröger M, Neukam FW. Osseointegration of endodontic endosseous cones: Zirconium oxide vs

titanium. *Oral Surgery, Oral Medicine, Oral Pathology, Oral Radiology, and Endodontics*. 2000;**89**(1):91-98

[109] Scarano A, Di Carlo F, Quaranta M, Piattelli A. Bone response to zirconia ceramic implants: An experimental study in rabbits. *The Journal of Oral Implantology*. 2003;**29**(1):8-12

[110] Sakthiabirami K, Vu VT, Kim JW, Kang JH, Jang KJ, Oh GJ, et al. Tailoring interfacial interaction through glass fusion in glass/zinc-hydroxyapatite composite coatings on glass-infiltrated zirconia. *Ceramics International*. 2018;**44**(14):16181-16190. Available from: <http://www.sciencedirect.com/science/article/pii/S0272884218313063>

[111] Osman RB, van der Veen AJ, Huiberts D, Wismeijer D, Alharbi N. 3D-printing zirconia implants; a dream or a reality? An in-vitro study evaluating the dimensional accuracy, surface topography and mechanical properties of printed zirconia implant and discs. *Journal of the Mechanical Behavior of Biomedical Materials*. 2017;**75**:521-528

[112] Cheng Y-C, Lin D-H, Jiang C-P, Lin Y-M. Dental implant customization using numerical optimization design and 3-dimensional printing fabrication of zirconia ceramic. *International Journal for Numerical Methods in Biomedical Engineering*. 2017;**33**(5):e2820

[113] Anssari Moin D, Hassan B, Wismeijer D. A novel approach for custom three-dimensional printing of a zirconia root analogue implant by digital light processing. *Clinical Oral Implants Research*. 2017;**28**(6):668-670. DOI: 10.1111/clr.12859

[114] Schwarzer E, Holtzhausen S, Scheithauer U, Ortmann C, Oberbach T, Moritz T, et al. Process development for additive manufacturing of functionally graded alumina toughened zirconia components intended for medical

implant application. *Journal of the European Ceramic Society*. 2019;**39**(2):522-530. Available from: <https://www.sciencedirect.com/science/article/pii/S095522191830548X>

[115] Zhu Y, Liu K, Deng J, Ye J, Ai F, Ouyang H, et al. 3D printed zirconia ceramic hip joint with precise structure and broad-spectrum antibacterial properties. *International Journal of Nanomedicine*. 2019;**14**:5977-5987

[116] Magnani G, Fabbri P, Leoni E, Salernitano E, Mazzanti F. New perspectives on zirconia composites as biomaterials. *Journal of Composites Science*. 2021;**5**(9):244. Available from: <https://www.mdpi.com/2504-477X/5/9/244>

[117] Sapkal PS, Kuthe AM, Mathankar S, Deshmukh AA. 3D bio-plotted tricalcium phosphate/zirconia composite scaffolds to heal large size bone defects. *Molecular & Cellular Biomechanics*. 2017;**14**(2):125-136. Available from: <https://www.proquest.com/scholarly-journals/3d-bio-plotted-tricalcium-phosphate-zirconia/docview/2397225089/se-2>

[118] Lin F, Yan C, Zheng W, Fan W, Adam C, Oloyede AK. Preparation of mesoporous bioglass coated zirconia scaffold for bone tissue engineering. *Advances in Materials Research*. 2012;**365**:209-215

[119] Kim Y-H, Lee B-T. Novel approach to the fabrication of an artificial small bone using a combination of sponge replica and electrospinning methods. *Science and Technology of Advanced Materials*. 2011;**12**(3):35002. DOI: 10.1088/1468-6996/12/3/035002

[120] Hadjicharalambous C, Buyakov A, Buyakova S, Kulkov S, Chatzinikolaidou M. Porous alumina, zirconia and alumina/zirconia for bone repair: Fabrication, mechanical and in

vitro biological response. *Biomedical Materials*. 2015;**10**(2):025012

[121] Jang D-W, Nguyen T-H, Sarkar SK, Lee B-T. Microwave sintering and in vitro study of defect-free stable porous multilayered HAp–ZrO<sub>2</sub> artificial bone scaffold. *Science and Technology of Advanced Materials*. 2012;**13**(3):35009. DOI: 10.1088/1468-6996/13/3/035009

[122] Mondal D, So-Ra S, Sarkar SK, Min YK, Yang HM, Lee BT. Fabrication of multilayer ZrO<sub>2</sub>–biphasic calcium phosphate–poly-caprolactone unidirectional channeled scaffold for bone tissue formation. *Journal of Biomaterials Applications*. 2012;**28**(3): 462-472

[123] Li Y, Li L, Li B. Direct write printing of three-dimensional ZrO<sub>2</sub> biological scaffolds. *Materials and Design*. 2015;**72**:16-20. Available from: <http://www.sciencedirect.com/science/article/pii/S0261306915000643>

[124] Shuai C, Feng P, Yang B, Cao Y, Min A, Peng S. Effect of nano-zirconia on the mechanical and biological properties of calcium silicate scaffolds. *International Journal of Applied Ceramic Technology*. 2015;**12**(6): 1148-1156

[125] Cadafalch Gazquez G, Chen H, Veldhuis SA, Solmaz A, Mota C, Boukamp BA, et al. Flexible yttrium-stabilized zirconia nanofibers offer bioactive cues for osteogenic differentiation of human mesenchymal stromal cells. *ACS Nano*. 2016;**10**(6): 5789-5799. DOI: 10.1021/acsnano.5b08005

[126] Sapkal PS, Kuthe AM, Kashyap RS, Nayak AR, Kuthe SA, Kawle AP. Indirect casting of patient-specific tricalcium phosphate zirconia scaffolds for bone tissue regeneration using rapid prototyping methodology. *Journal of Porous Materials*. 2017;**24**(4):1013-1023. DOI: 10.1007/s10934-016-0341-6

[127] Thakare VG, Joshi PA, Godse RR, Bhatkar VB, Wadegaokar PA, Omanwar SK. Fabrication of polycaprolactone/zirconia nanofiber scaffolds using electrospinning technique. *Journal of Polymer Research*. 2017;**24**(12):232. DOI: 10.1007/s10965-017-1388-z

[128] Stanciuc A-M, Sprecher CM, Adrien J, Roiban LI, Alini M, Gremillard L, et al. Robocast zirconia-toughened alumina scaffolds: Processing, structural characterisation and interaction with human primary osteoblasts. *Journal of the European Ceramic Society*. 2018;**38**(3):845-853. Available from: <http://www.sciencedirect.com/science/article/pii/S0955221917305708>

[129] Sa M-W, Nguyen B-NB, Moriarty RA, Kamalidinov T, Fisher JP, Kim JY. Fabrication and evaluation of 3D printed BCP scaffolds reinforced with ZrO<sub>2</sub> for bone tissue applications. *Biotechnology & Bioengineering*. 2018;**115**(4):989-999. DOI: <https://doi.org/10.1002/bit.26514>

[130] Brazete D, Neto AS, Ferreira JMF. Optimization of zirconia inks to fabricate 3D porous scaffolds by robocasting. *LEK Technology*. 2019;**49**(1):5-10

[131] Fu SY, Yu B, Ding HF, Shi GD, Zhu YF. Zirconia incorporation in 3D printed  $\beta$ -Ca<sub>2</sub>SiO<sub>4</sub> scaffolds on their physicochemical and biological property. *Wuji Cailiao Xuebao/ Journal of Inorganic Materials*. 2019;**34**(4):444-454

[132] Zhang J, Huang D, Liu S, Dong X, Li Y, Zhang H, et al. Zirconia toughened hydroxyapatite biocomposite formed by a DLP 3D printing process for potential bone tissue engineering. *Materials Science and Engineering: C*. 2019;**105**: 110054. Available from: <http://www.sciencedirect.com/science/article/pii/S0928493119310537>

- [133] Wang Q, Ma Z, Wang Y, Zhong L, Xie W. Fabrication and characterization of 3D printed biocomposite scaffolds based on PCL and zirconia nanoparticles. *Bio-Design and Manufacturing*. 2021;**4**(1):60-71. DOI: 10.1007/s42242-020-00095-3
- [134] Cao Y, Shi T, Jiao C, Liang H, Chen R, Tian Z, et al. Fabrication and properties of zirconia/hydroxyapatite composite scaffold based on digital light processing. *Ceramics International*. 2020;**46**(2):2300-2308. Available from: <http://www.sciencedirect.com/science/article/pii/S0272884219327567>
- [135] Kocyło E, Franchin G, Colombo P, Chmielarz A, Potoczek M. Hydroxyapatite-coated ZrO<sub>2</sub> scaffolds with a fluorapatite intermediate layer produced by direct ink writing. *Journal of the European Ceramic Society*. 2021;**41**(1):920-928. Available from: <http://www.sciencedirect.com/science/article/pii/S0955221920306634>
- [136] Lee BT, Kang IC, Cho SH, Song HY. Fabrication of a continuously oriented porous Al<sub>2</sub>O<sub>3</sub> body and its in vitro study. *Journal of the American Ceramic Society*. 2005;**88**(8):2262-2266
- [137] Wei C, Montagnac G, Reynard B, Le Roux N, Gremillard L. Interplay between internal stresses and matrix stiffness influences hydrothermal ageing behaviour of zirconia-toughened-alumina. *Acta Materialia*. 2020;**185**:55-65. Available from: <https://www.sciencedirect.com/science/article/pii/S1359645419308018>
- [138] Reginato VF, Kemmoku DT, Caldas RA, Bacchi A, Pfeifer CS, Consani RLX. Characterization of residual stresses in veneering ceramics for prostheses with zirconia framework. *Brazilian Dental Journal*. 2018;**29**(4): 347-353
- [139] Zhang Y, Allahkarami M, Hanan JC. Measuring residual stress in ceramic zirconia–porcelain dental crowns by nanoindentation. *Journal of the Mechanical Behavior of Biomedical Materials*. 2012;**6**:120-127. Available from: <https://www.sciencedirect.com/science/article/pii/S1751616111002931>
- [140] Jang K-J, Kang J-H, Sakthiabirami K, Lim H-P, Yun K-D, Yim E-K, et al. Evaluation of cure depth and geometrical overgrowth depending on zirconia volume fraction using digital light processing. *Journal of Nanoscience and Nanotechnology*. 2018;**19**(4): 2154-2157
- [141] Kosyfaki P, del Pilar Pinilla Martín M, Strub JR. Relationship between crowns and the periodontium: A literature update. *Quintessence International*. 2010;**41**(2):109-126
- [142] Contrepolis M, Soenen A, Bartala M, Laviolle O. Marginal adaptation of ceramic crowns: A systematic review. *The Journal of Prosthetic Dentistry*. 2013;**110**(6):447-454.e10
- [143] 10 of the Biggest Challenges in Scaling Additive Manufacturing for Production in 2020 [Expert Roundup]—AMFG. Available from: <https://amfg.ai/2019/10/08/10-of-the-biggest-challenges-in-scaling-additive-manufacturing-for-production-expert-roundup/>